Gondwana Research 17 (2010) 662–675

Contents lists available at ScienceDirect

Gondwana Research

journal homepage: www.elsevier.com/locate/gr

The southern segment of the Famatinian magmatic arc, La Pampa Province, Argentina

Carlos J. Chernicoff [a,b,*], Eduardo O. Zappettini [b], João O.S. Santos [c,d], Shelley Allchurch [e], Neal J. McNaughton [c]

[a] Council for Scientific and Technical Research (CONICET), Argentina
[b] Argentine Geological-Mining Survey (SEGEMAR), Argentina
[c] University of Western Australia, Australia
[d] Redstone Resources, Australia
[e] ARC National Key Centre for Geochemical Evolution and Metallogeny of Continents (GEMOC), Macquarie University, Sydney, Australia

ARTICLE INFO

Article history:
Received 30 September 2008
Received in revised form 28 October 2009
Accepted 30 October 2009
Available online 29 November 2009

Keywords:
Famatinian magmatic arc
U–Pb SHRIMP
Hf isotopes
Aeromagnetics
La Pampa
Argentina

ABSTRACT

The present study led to the identification of a largely hidden southern segment of the Famatinian magmatic arc in the province of La Pampa, south-central Argentina. The arc is represented by scarce outcrops of metaigneous rocks (mostly meta-quartz-diorites and metagabbros) but stands out in the aeromagnetic data as a conspicuous and continuous, NNW-trending magnetic anomaly. The geochemical signature of this magmatic suite points to a pre-collisional continental magmatic arc. Its crystallization age (U–Pb SHRIMP dating on magmatic zircon) ranges from ca. 476 to 466 Ma, being comparable, therefore, to the central and northern segments of the Famatinian arc. All dated zircon of the metagabbro have similar $^{176}Hf/^{177}Hf$ ratios, negative ε_{Hf} (from −5.02 to −3.62) and average Lu–Hf model ages of ca. 1.7 Ga, indicating a crustal contamination of a mantle-derived mafic magma (of ca. 466 Ma) with much older rocks, probably older than 2 Ga, hence suggesting that part of the underlying basement of the southernmost Pampia terrane is at least this old. U–Pb SHRIMP dating on metamorphic zircon rims/areas yielded ca 454 Ma, that is within the 465–450 Ma age range of Famatinian metamorphism previously recorded in La Pampa. The amphibolite-facies metamorphism that affects the magmatic arc in La Pampa is attributed to the collision of the Cuyania (greater Precordillera) terrane against the western margin of Gondwana.

1. Introduction

Early Paleozoic east-dipping subduction of Iapetus oceanic lithosphere beneath the proto-Andean margin of western Gondwana gave rise to the Famatinian magmatic arc (Pankhurst et al., 1998; Quenardelle and Ramos, 1999; Pankhurst et al., 2000), that preceded the amalgamation of the allochthonous Precordillera terrane in mid-Ordovician times (e.g. Astini et al., 1995).

The Famatinian magmatic arc is mainly exposed in central and northern Argentina (e.g. Saavedra et al., 1992; Loske and Miller, 1996; Pankhurst et al., 1998; Pankhurst and Rapela, 1998; Rapela et al., 1998; Poma and Zappettini, 1998; Bahlburg, 1998; Stuart-Smith et al., 1999; Pankhurst et al., 2000; von Gosen et al., 2002; Coira and Koukharsky, 2002; Toselli et al., 2002; Zimmermann and Bahlburg, 2003; Sato et al., 2003; Astini and Dávila, 2004; Varela et al., 2008; Dahlquist et al., 2008). Its continuation in south-central Argentina (La Pampa province; Fig. 1), a topographically flat region largely covered by Quaternary sediments, was proposed by Villar et al. (2005) and Chernicoff et al. (2008d,e, 2009). Aeromagnetic data were a key tool for the delineation of the southern segment of the arc. In this region, the arc is represented by scarce outcrops exposed along the Chadileuvú River bed including meta-quartz-diorites at Paso del Bote and metagabbros at Urre Lauquen, as well as late tectonic granodiorites at Estancia El Trabajo (Fig. 1).

In this article we present zircon U–Pb SHRIMP data and Hf isotope compositions of the main rock types of the Famatinian magmatic arc at this latitude, together with their geochemical and geophysical signatures. The results are discussed in the context of the Lower Paleozoic evolution of the southwestern margin of Gondwana.

2. Methods of investigation

Since the area of investigation is extensively covered by Quaternary sediments that largely obscure the basement units, aeromagnetic data for this region, provided by the Geological Survey of Argentina (SEGEMAR, 2005), were analyzed, resulting in a broad geological–geotectonic interpretation (Chernicoff and Zappettini, 2003, 2004). Salient anomalies were checked during field trips in 2003 and 2005.

A selection of the collected samples was used for petrographic studies at SEGEMAR. Unaltered and homogeneous samples were selected for chemical analyses, which were performed at Activation Laboratories Ltd. of Canada. Major elements were analyzed by ICP and

* Corresponding author. Council for Scientific and Technical Research (CONICET), Argentina. Tel.: +54 11 4349 3099; fax: +54 11 4349 3171.
E-mail address: jchern@secind.mecon.gov.ar (C.J. Chernicoff).

1342-937X/$ – see front matter © 2009 International Association for Gondwana Research. Published by Elsevier B.V. All rights reserved.
doi:10.1016/j.gr.2009.10.008

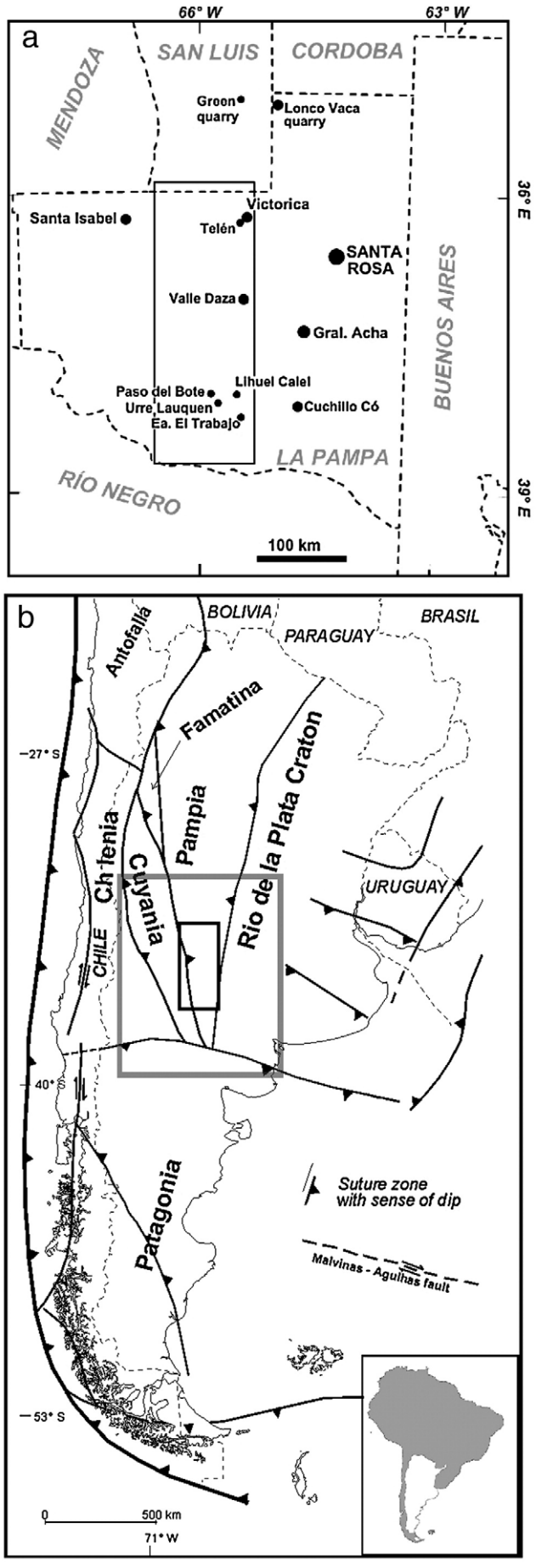

trace element by ICP/MS. Procedures may be found at www.actlabs.com.

Zircon grains separated from the rock samples were first analyzed by SEM (scanning electron microscope) at the Centre for Microscopy, Characterization and Microanalyses at the University of Western Australia, Perth.

U–Pb analyses were carried out at Curtin University of Technology, Perth, and the Hf isotopic analyses at Macquarie University, Sydney. The combination of all the data obtained allowed preparation of a basement geological map for the study region. Geophysical maps and modeling of aeromagnetic data were prepared using commercial software packages proprietary to SEGEMAR.

3. Geological setting

The basement of the study region (La Pampa province, south-central Argentina; Fig. 1), comprises the southern portion of the Pampia (Eastern Sierras Pampeanas) and Cuyania (greater Precordillera) terranes, amalgamated to the western margin of Gondwana during the Cambrian and Middle Ordovician, respectively (see e.g. Astini et al., 1996; Pankhurst et al., 1998; Thomas and Astini, 2003; Ramos, 2004, and references therein; Gregori et al., 2008; Casquet et al., 2008, and references therein). The boundaries between these terranes in south-central Argentina were defined by Chernicoff and Zappettini (2003, 2004), largely on the basis of aeromagnetic data. These authors also draw the boundary between Pampia and the Río de la Plata craton roughly at 65° W, indicating that the easternmost portion of the basement of La Pampa province corresponds to the autochtonous Precambrian basement of Gondwana (Río de La Plata craton), as suggested by Ramos (1996).

The Cuyania–Pampia terrane boundary is delineated by a large NNW-trending positive magnetic anomaly. Ground checking of this anomaly indicates that it coincides with local outcrops of mainly meta-quartz-diorites and metagabbros at Paso del Bote and Ure Lauquen, and late tectonic granodiorites at Estancia El Trabajo. This suggests that the full extent of the anomaly arises from similar, unexposed, metaigneous rocks, forming a single NNW-trending belt. These rocks lie on the Pampia side (upper plate) of the Cuyania–Pampia suture zone, and would represent the southernmost Famatinian magmatic arc. U–Pb SHRIMP dating of these rocks presented in this paper yield crystallization ages of ca 476 to 466 Ma. Both the magnetic anomaly and the suture terminate abruptly at the northern margin of the Patagonia terrane (Chernicoff and Zappettini, 2003, 2004).

To the east of the Cuyania–Pampia suture and within the Pampia terrane, evidence for a Famatinian magmatic back-arc comes from a belt of metagabbros, scarcely exposed at Valle Daza and Sierra de Lonco Vaca (La Pampa province), which also gives rise to a large and conspicuous, roughly N–S-trending positive magnetic anomaly. These metagabbros have a MORB geochemical signature and their (U–Pb SHRIMP) age is 450 ± 4 Ma (Chernicoff et al., 2008c). Chernicoff et al. (2009) have compared these metagabbros with the Lower Paleozoic mafic–ultramafic rocks of the Sierra de San Luis.

The host rocks of the Famatinian magmatic arc (and back-arc) at the latitude of La Pampa are quartz–plagioclase–biotite schists to gneisses of sedimentary protolith whose maximum depositional age has been established at ca. 500 to 515 Ma (Chernicoff et al., 2007, 2008b). Deposition of these sediments probably occurred during the Upper Cambrian–Lower Ordovician, making them possible equivalents of the metasedimentary rocks of the Pringles Metamorphic Complex (Sims et al., 1998) of the Sierra de San Luis. Regional metamorphism of these sediments (and associated igneous bodies) started at ca 465/461 Ma (ca.

Fig. 1. a) Locality map of the study area (inner rectangle; see also Fig. 11 for geophysical coverage) and surrounding provinces of south-central Argentina. b) Study area and greater region in the context of the map of accreted terranes in southern South America (slightly modified after Chernicoff and Zappettini, 2004).

Table 1
Chemical analyses of the Famatinian metaigneous rocks of Paso del Bote and surroundings, La Pampa province.

Sample	81	78C	79A	44A	43A	79D	82	75A	75B	105	110A	111
Locality	PB	PB	PB	PB	PB	PB	PB	UL	UL	EET	EET	EET
Lithology	mGb-Dt	mGb-Dt	mD	mqD	mTn	mGr	Sd	mGb	mGb	mGd	mGd	mGr
Lat (S)	38.02412	38.02833	38.02725	38.02732	38.0281	38.02725	38.02412	38.12	38.1182	38.23778	38.24815	38.23527
Long (W)	65.8241	65.8187	65.82065	65.82077	65.81915	65.82065	65.82403	65.7621	65.7621	65.34648	65.44795	65.33428
SiO2	48.82	51.97	51.79	56.26	59.36	68.55	55.03	51.42	52.22	66.12	75.87	68.43
TiO2	1051	1115	1.1	0.959	0.806	0.245	0.836	1258	0.552	0.528	0.058	0.527
Al2O3	13.98	17.85	17.88	16.98	16.64	14.45	14.52	14.13	4.67	14.92	13.31	14.3
Fe2O3(T)	12.3	9.82	9.32	8.35	6.8	2.2	6.06	13.4	12.75	3.65	0.37	3.66
MnO	0.202	0.174	0.169	0.178	0.146	0.046	0.105	0.291	0.442	0.07	0.013	0.06
MgO	7.05	4.03	3.98	4.17	3.29	0.69	3.29	6.5	15.94	2.1	0.1	1.7
CaO	8.57	8.03	7.5	5.83	5.06	2.28	6.11	9.22	11.26	3.45	1.11	1.46
Na2O	2.7	2.77	2.87	2.66	2.59	3.31	3.74	0.96	0.55	3.43	3.69	2.8
K2O	2.59	1.6	1.64	2.01	1.7	5.82	3.34	1.47	0.43	3.93	4.81	5.34
P2O5	0.12	0.16	0.12	0.2	0.15	0.09	0.39	0.12	0.04	0.18	0.04	0.19
LOI	2.45	3.09	2.33	2.54	3.23	2.27	6.85	1.98	1.73	1.61	0.68	1.71
Total	99.83	100.6	98.69	100.1	99.76	99.96	100.3	100.7	100.6	99.97	100.1	100.2
Ba	572	311	302	302	387	1336	1112	289	31	1098	367	902
Rb	88	41	55	80	79	144	100	56		115	202	231
Sr	184	238	230	194	189	248	311	128	25	511	130	331
Cs	2.1	3.3	3.1	3.2	5	2	3.4	6.9		4.2	11.8	8
Ga	18	21	19	22	18	14	17	19	10	19	18	20
Tl	0.7	0.4	0.3	0.8	0.5	1.3	1.2	0.7		0.8	1.7	2
Ta	0.5	0.5	0.6	0.7	0.7	1.6	0.7	0.3	0.2	0.8	3.2	1.4
Nb	6	9	9	9	9	6	12	3	3	11	15	18
Hf	2.1	3.6	3.6	4.2	3.9	3.4	4.4	2	2.4	5.3	1.9	8.2
Zr	73	120	125	147	143	117	182	71	66	196	38	298
Y	26	29	32	28	27	6	14	27	26	17	8	25
Th	0.6	5.6	5.1	11	1.2	2.6	9.9	0.8	2	19.7	19.7	54.3
U	0.4	0.9	0.9	0.6	0.6	0.8	1.7	0.4	0.8	2.2	3.2	3.9
Cr	90		< 20	40	30		200	90	1010	50		40
Ni	70	20	< 20	30	< 20		80	80	170	30		30
Co	64	63	22	68	17	113	30	70	62	97	158	74
Sc	46	25	25	25	19	6	13	45	83	10	2	8
V	360	237	230	208	149	55	123	413	300	77	18	85
Cu	70	50	40	40	20	30		100	50			170
Pb	7	29	13	22	16	47	45	11	15	44	75	57
Zn	100	100	60	110	70		70	130	280	50		50
Bi	0.8	1.2	<0.4	0.5	<0.4	1.6		3.7	16.5	0.5	1.3	40.4
In			<0.2		<0.2				0.8			
Sn	2	3	2	3	4		1	2	3	2		3
Mo			<2		<2							
Be	3	2	2	3	3	3	2	2	2	3	8	4
Ag	0.6		<0.5		<0.5	0.8						
Ge	2	1		2		1		2	3		1	1
As	5					5			8			
Sb		0.6		0.8			0.5	1.9	1.8	2	1.4	0.5
La	8.4	19.7	17.9	28	10.6	11.1	42.3	4	8.7	50.9	13.1	80.8
Ce	22	48.7	42.6	66.3	23.5	24.4	83.4	11.5	25.4	101	27.3	158
Pr	2.91	5.94	5.36	7.26	3.08	2.52	9.17	1.7	3.67	10.5	2.82	16
Nd	13	24.9	21.9	28.6	14.3	9	33.3	9.2	18.1	37.3	9.8	54.3
Sm	3.4	5.9	5.1	6.3	3.7	1.7	6	3	5.5	6.4	1.9	9.3
Eu	1.09	1.26	1.18	1.38	1.03	0.87	1.43	1.13	0.92	1.38	0.33	1.46
Gd	4.1	5.5	5.1	5.5	4.1	1.5	4.7	3.8	5.4	5.1	1.6	7.1
Tb	0.8	0.9	0.9	0.9	0.8	0.2	0.6	0.7	0.9	0.6	0.2	0.9
Dy	4.7	4.9	5.1	5.2	4.5	1.1	2.9	4.4	5.2	3.1	1.3	4.3
Ho	1	1	1	1	0.9	0.2	0.5	1	1	0.6	0.3	0.8
Er	3	3	3	3.1	2.7	0.5	1.6	2.9	2.9	1.7	0.9	2.5
Tm	0.45	0.46	0.45	0.47	0.4	0.07	0.23	0.44	0.44	0.26	0.14	0.38
Yb	2.9	2.9	2.8	3	2.5	0.5	1.5	2.9	2.7	1.7	1.1	2.4
Lu	0.43	0.43	0.41	0.44	0.32	0.08	0.21	0.42	0.4	0.24	0.17	0.34
CIPW NORM												
Q (S)	0	6.69	6.68	13.53	21.86	22.17	6.02	11.52	6.15	21.31	33.75	26.31
or (KAS6)	15.85	9.76	10.12	12.24	10.46	35.29	21.23	8.87	2.59	23.68	28.64	32.15
ab (NAS6)	23.6	24.15	25.31	23.15	22.77	28.67	33.96	8.28	4.74	29.53	31.39	24.08
an (CAS2)	18.97	32.49	32.36	28.59	25.21	7.51	13.89	30.47	9.16	13.92	5.31	6.24
lc (KAS4)	0	0	0	0	0	0	0	0	0	0	0	0
ne (NAS2)	0	0	0	0	0	0	0	0	0	0	0	0
C (A)	0	0	0	0.24	1.71	0	0	0	0	0	0.08	1.68
ac (NFS4)	0	0	0	0	0	0	0	0	0	0	0	0
ns (NS)	0	0	0	0	0	0	0	0	0	0	0	0
Di wo (CS)	10.14	3.2	2.4	0	0	1.48	6.78	6.48	19.85	1.02	0	0
Di en (MS)	7.79	2.06	1.57	0	0	0.88	4.75	4.27	14.94	0.73	0	0
Di fs (FS)	1.26	0.91	0.66	0	0	0.52	1.45	1.74	2.87	0.2	0	0

Table 1 (*continued*)

Sample	81	78C	79A	44A	43A	79D	82	75A	75B	105	110A	111
Locality	PB	PB	PB	PB	PB	PB	PB	UL	UL	EET	EET	EET
Lithology	mGb-Dt	mGb-Dt	mD	mqD	mTn	mGr	Sd	mGb	mGb	mGd	mGd	mGr
CIPW NORM												
Hy en (MS)	5.42	8.33	8.81	10.73	8.56	0.89	4.09	12.32	25.68	4.62	0.25	4.33
Hy fs (FS)	0.88	3.69	3.7	3.93	3.2	0.53	1.25	5.01	4.93	1.3	0.15	1.5
Ol fo (M2S)	3.51	0	0	0	0	0	0	0	0	0	0	0
Ol fa (F2S)	0.63	0	0	0	0	0	0	0	0	0	0	0
mt (FF)	9.61	6.18	5.93	5.26	4.31	1.38	3.97	8.35	7.94	2.27	0.23	2.27
he (F)	0	0	0	0	0	0	0	0	0	0	0	0
il (FT)	2.07	2.19	2.18	1.88	1.59	0.48	1.71	2.44	1.07	1.02	0.11	1.02
ap (CP)	0.27	0.36	0.27	0.45	0.34	0.2	0.91	0.27	0.09	0.4	0.09	0.42

PB: Paso del Bote; UL: Urre Lauquen; EET: Estancia El Trabajo; mGb: metagabbro; mGb-Dt: metagabbro-diorite; mDt: metadiorite; mTn: metatonalite; mQD: meta-quartz-diorite; mGd: metagranodiorite; mGr: metagranite; Sd: syenodiorite.
Geographic coordinates in Gauss Kruger projection.

465 Ma: U–Pb SHRIMP age, Chernicoff et al., 2008a; ca. 461 Ma: Ar–Ar age, Tickyj et al., 1999) and continued to ca 450 Ma, as recorded both in the Famatinian back-arc metagabbros of Valle Daza, La Pampa (U–Pb SHRIMP; Chernicoff et al., 2008c) and in the Sierra de San Luis (U–Pb; Sims et al., 1998). Similar age ranges of metamorphism have also been reported from several outcrops in the Sierras Pampeanas (e.g. Rapela et al., 2001; Casquet et al., 2001; Baldo et al., 2001; Vujovich et al., 2004), which are possibly related to the collision of the Cuyania terrane to the western margin of Gondwana.

On the Cuyania side of the Cuyania–Pampia terrane divide, the depocentre of a Late Ordovician–Devonian marine foreland basin generated after the Middle Ordovician collision of Cuyania – the Curacó basin – is conspicuously delineated by a narrow NNW-oriented magnetic low. It comprises sandstones and shales of the La Horqueta Formation, representing the southern continuation of the same unit exposed in the San Rafael Block of Cuyania (Chernicoff et al., 2008d). According to these authors, the geochemical signature of these sediments indicates derivation from an active continental margin, possibly corresponding to the Famatinian arc.

4. Petrography

Very scarce outcrops of metadiorites, meta-quartz-diorites grading to metagabbro-diorites and metatonalites, as well as metagranites and a small number of dikes of aplitic to bostonitic texture, ranging in composition from granodiorite to syenodiorite, are exposed along the Chadileuvú River bed at Paso del Bote. Individually, each exposure occupies a surface not larger than 20 m^2, locally extending for 1.2 km. The dikes stand out slightly on the flat surface of the outcrops. About 10 km to the southeast of Paso del Bote, an exiguous exposure of metagabbros is located by the shore of the Urre Lauquen pond (Fig. 1a; see also Fig. 11b). In addition, 25 km to the southeast of Urre Lauquen, late tectonic granodiorites to monzogranites scarcely crop out at Estancia El Trabajo (Fig. 1a; see also Fig. 11b). The full extent of the Famatinian magmatic arc rocks in La Pampa, defined later in the text, forms a ca. 270 km long–20 km wide NNW-trending belt, i.e. including sub-outcrops and areas of thin sedimentary cover, as inferred from aeromagnetics (see GEOPHYSICS, below).

Foliation planes strike N–S to NNW and dip subvertically. Although detailed structural measurements cannot be done due to the nature of the exposures, a NNW regional structural trend is also shown by the aeromagnetic data (see Fig. 11a).

Most of the metaigneous rock types exposed at Paso del Bote are dark greenish grey in colour, and mostly coarse grained. The meta-quartz-diorites are the main rock type, with local variations to gabbrodioritic and tonalitic compositions. Metagranites also occur in this area.

The meta-quartz-diorites exhibit coarse-grained granonematoblastic texture, comprising hornblende, plagioclase (andesine), scarce biotite and quartz; zircon and apatite are the accessory minerals. They reached amphibolite-facies regional metamorphism, represented by the hornblende–plagioclase–biotite association; granonematoblastic texture and foliation were developed at this stage. Ductile deformation under greenschist-facies metamorphic conditions followed, with neoformation of chlorite (replacing hornblende), albite (replacing andesine), epidote, tremolite and sphene; often, quartz and albite are finely recrystallized, replacing hornblende. During this stage, mylonitization affected the rock assemblage, mostly concentrated in narrow N–S-trending belts; in the mylonitized rocks chlorite is aligned along the mylonitic texture, plagioclase is rotated and curved, and quartz is fragmented and tends to form ribbon-like structures. Finally, under fragile conditions microfracturing and hydrothermal alteration took place, represented by carbonate veinlets, disseminated opaque minerals, propylitization and sericitization.

The gabbrodioritic variety is characterized by the largely argillized and sericitized plagioclase of andesine–labradorite normative composition, and preservation of relics of clinopyroxene. In the tonalitic variety, magmatic hornblende is almost completely replaced by chlorite.

The metagranites exhibit coarse-grained granoblastic texture comprising quartz, microcline, minor sericited oligoclase, locally showing antiperthitic texture, scarce biotite replaced by chlorite, and epitote; zircon, apatite and opaques are the accessory minerals.

The dikes are less than 1 m thick and trend NS (i.e. roughly parallel to the foliation of the metaigneous rocks), exhibiting aplitic to bostonitic textures, and varying compositionally between granodiorite to syenodiorite. The granodioritic dikes consist of euhedral oligoclase, quartz, microcline and muscovite. The syenodioritic dikes consist essentialy of laths of alkali-feldspar and plagioclase (oligoclase–andesine), and minor mafic minerals altered to chlorite and carbonate, as well as scarce interstitial quartz; the accessory minerals are sphene, opaques and minor apatite.

At outcrop scale, the metagabbros of Urre Lauquen differ from the metaigneous rock types of Paso del Bote by their black colour and more massive aspect. The metagabbros exhibit coarse-grained granonematoblastic texture comprising plagioclase (labradorite) and clinopyroxene (diopside–augite); sphene and zircon are the accessory minerals. Clinopyroxene is mostly replaced by hornblende during amphibolite-facies metamorphism. The superimposed, greenschist-facies metamorphism is evidenced by the transition of hornblende to epidote and tremolite–actinolite, and by the formation of albite and chlorite at the expense of calcic plagioclase.

At Estancia El Trabajo there are medium-grained granodiorites grading to monzogranites, consisting of euhedral to subhedral crystals of zoned oligoclase locally showing mirmekitic texture, anhedral quartz, subhedral hornblende partially chloritized and biotite; microcline is partially argillized and locally exhibits graphic texture; accessory minerals are sphene, opaques, apatite and zircon. Secondary epidote and calcite could represent a propylitic alteration related to Permo-Triassic eruptive activity close to the area. At this site, the granodiorites–monzogranites are less affected by metamorphism only evidenced by local shearing.

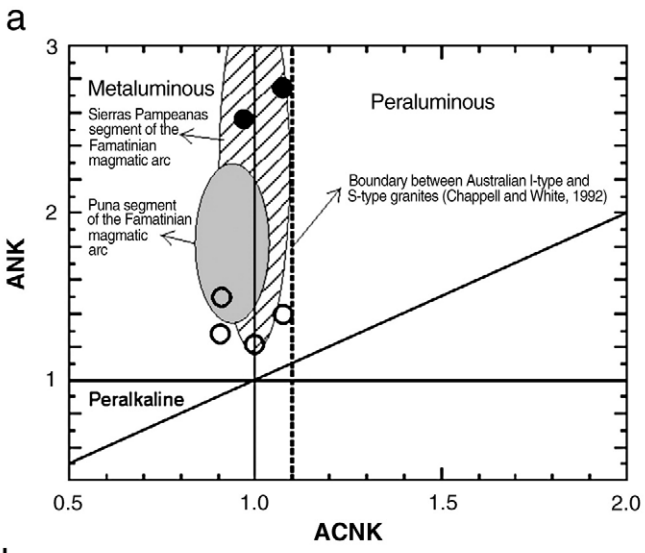

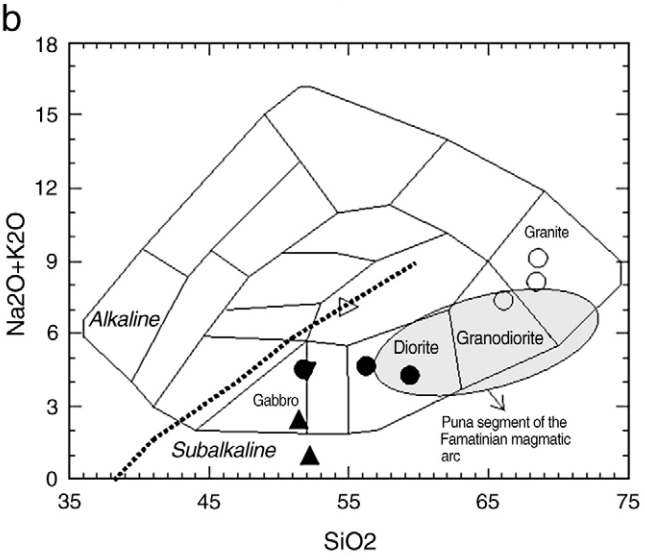

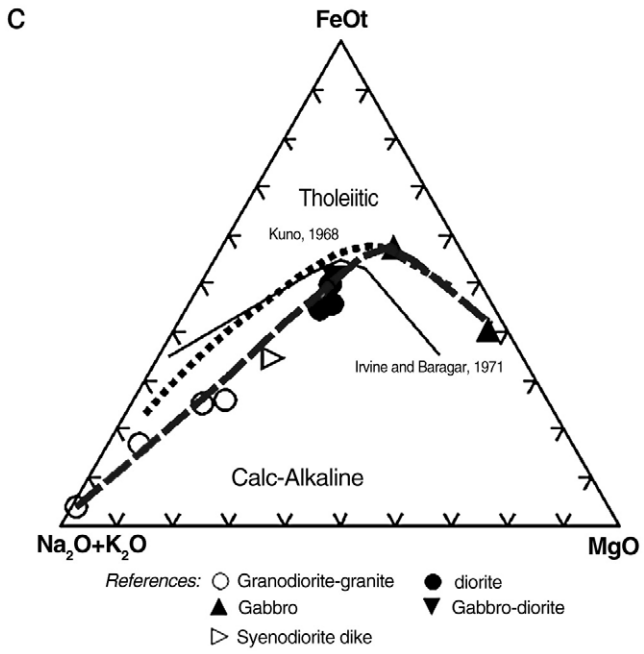

Fig. 2. a) Plots of $Al_2O_3/(Na_2O+K_2O)$ versus $Al_2O_3/(CaO+Na_2O+K_2O)$ for the La Pampa Famatinian arc rocks. Areas for Sierras Pampeanas and Puna segment of the Famatinian arc are indicated for comparison. b) Plots of the La Pampa Famatinian arc rocks in the total alkalis versus silica (TAS) diagram of Cox et al. (1979) adapted by Wilson (1989) for plutonic rocks. The area for the Puna segment of the Famatinian arc is indicated for comparison. c) AFM diagram after Irvine and Baragar (1971) showing the La Pampa Famatinian arc rock compositions and trend.

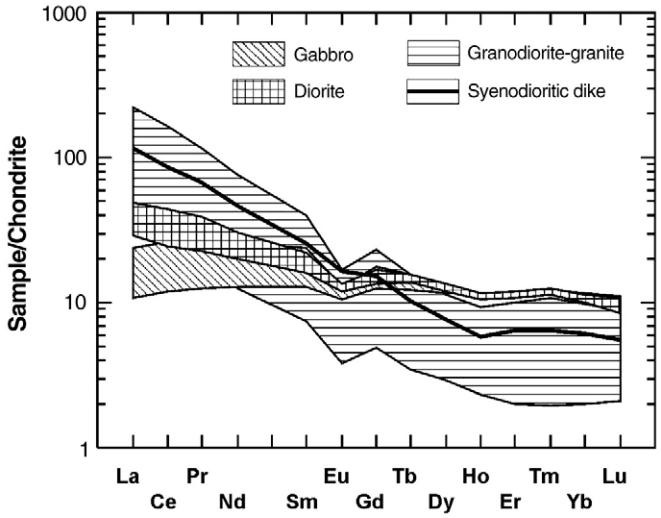

Fig. 3. Chondrite-normalized REE patterns of McDonough and Sun (1995) applied to the La Pampa Famatinian arc rocks.

5. Chemistry

Chemical analyses of the main lithologic types identified at Paso del Bote, Urre Lauquen and Estancia El Trabajo are given in Table 1.

For most major elements (TiO_2, Fe_2O_3, Al2O3, CaO and MnO) the analyzed rocks show negative correlation with SiO_2 and coherent trends that can be explained by continuous crystal fractionation of the principal rock-forming minerals. Na_2O and K_2O show a positive correlation with SiO2, most samples falling in the high-K field. P_2O_5 shows a trend with negative correlation for samples with SiO_2>55%, similar to what was found by Pankhurst et al. (1998) in the Famatinian granitoids from La Rioja. Following Green and Watson (1982), and given the high-K character of the granitoids, the P_2O_5 behaviour is interpreted as a case of calc-alkaline series poor in phosphorus.

Major elements indicate a metaluminous to marginally peraluminous character (Fig. 2a) and are very similar geochemically to some of the (Famatinian) magmatic arc field defined to the north (e.g. Pankhurst et al., 1998; Poma et al., 2004).

They are subalkaline rocks with SiO_2 contents ranging between 51 and 76%, and Al_2O_3 from 13.3 to 17% (Fig. 2b) and all the studied metaigneous rocks are subalkaline.

In the AFM diagram, the studied rocks form a calc-alkaline trend (Fig. 2c).

The chondrite-normalized REE patterns show enrichment in light REE, reflecting the crustal contamination typical of these types of rocks (Fig. 3). The REE pattern of the most primitive unit (Urre Lauquen metagabbro) is relatively flat, with no Eu anomaly, whereas the more evolved variety shows a negative Eu anomaly that indicates a derivation by plagioclase fractionation due to contamination with continental crust. The diagram shows a gradual increase in LREE/HREE ratio from gabbroic to granodioritic–granitic compositions. The more acidic types show the characteristic pattern of crustal rocks.

The Rb versus Y + Nb tectonic discriminant diagram points to a pre-collisional magmatic arc (Fig. 4a). Analyzed samples plot in the field previously defined for the northern part of the Famatinian arc (e.g. Pankhurst et al., 1998; Poma et al., 2004). The metagabbros of

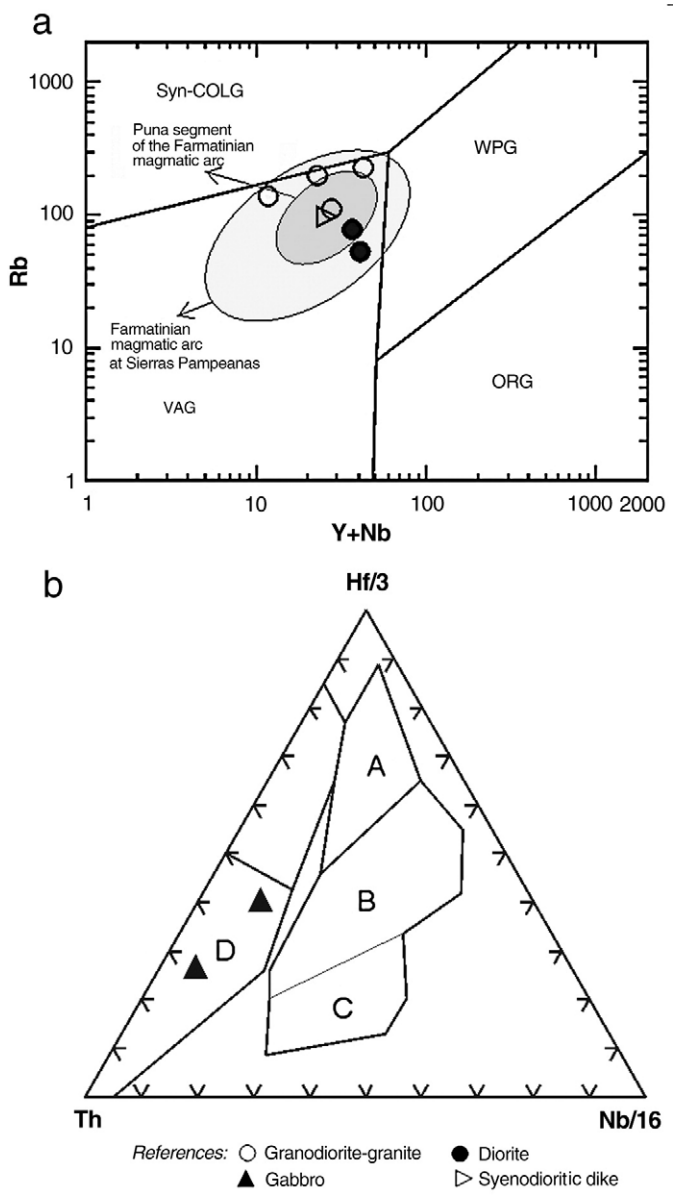

Fig. 4. a) Plots of La Pampa Famatinian arc rocks in the Rb (ppm) versus Y + Nb (ppm) discrimination diagram (Pearce et al., 1984). Areas for Sierras Pampeanas (Pankhurst et al., 1998) and Puna segment (Poma et al., 2004) of the Famatinian arc are indicated for comparison. b) Plots of La Pampa Famatinian arc rocks in the Th–Hf/3-Nb/16 discrimination diagram of Wood (1980). All samples plot in the D (calc-alkaline arc basalts) field.

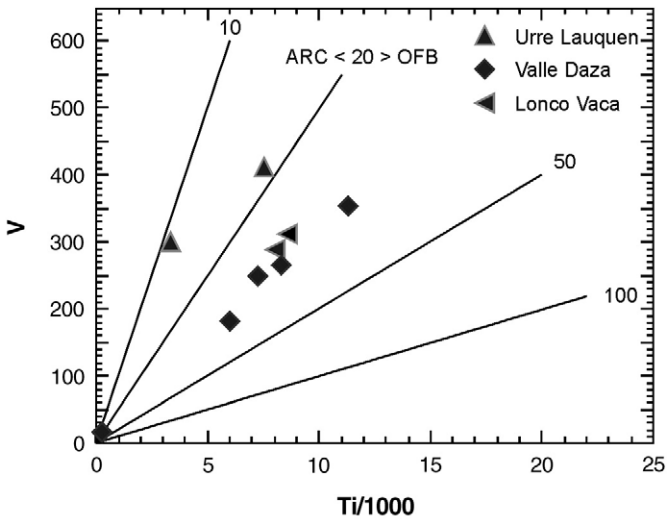

Fig. 5. V versus Ti/1000 diagram of Shervais (1982) applied to the La Pampa Famatinian arc gabbros of Urre Lauquen. The La Pampa back-arc gabbros (Valle Daza and Lonco Vaca outcrops) are shown for comparison.

this suite fall within the calc-alkaline basalts field in the Th–Hf/3-Nb/16 ternary diagram (Fig. 4b).

The metagabbros from Urre Lauquen (study area, see Fig. 1) and the MORB-type metagabbros of Valle Daza and Sierra de Lonco Vaca (Chernicoff et al., 2009) are clearly different in Ti/V discrimination diagram (Shervais, 1982): the former plot in the arc tholeiite field and the latter in the ocean floor basalt field (Fig. 5).

6. Geochronological data

6.1. U–Pb SHRIMP dating

6.1.1. Methodology

Samples MG44 (meta-quartz-diorite) and MG75a (metagabbro) were collected at Paso del Bote and Urre Lauquen, respectively (see Fig. 1). The rocks were crushed, milled, sieved at 60 mesh, and washed to remove the clay and silt fractions. The remaining material, corresponding to fine sand and very fine sand, was dried and processed by two heavy liquids: LST (lithium–sodium tungstate, density 2.8) and TBE (tetra-bromo-ethane, density 3). The heavy mineral concentrates were separated into four fractions using a Frantz® magnetic separator. Zircon was picked from the least magnetic fraction at 1 A and 5° inclination and then mounted in an epoxy disc of 2.5 cm diameter together with the analytical standards. The mount was polished and coated with carbon for imaging using a JEOL6400 Scanning Electron Microscope at the Centre for Microscopy, Characterization and Microanalyses of the University of Western Australia. This carbon coating was removed and replaced for a gold coating for SHRIMP U–Pb analyses.

Sensitive High Mass Resolution Ion MicroProbe (SHRIMP II) U–Pb analyses were performed at Curtin University of Technology in two sessions, using an analytical spot size of about 20–25 μm. Individual analyses are composed of nine measurements (Zr_2O, ^{204}Pb, background, ^{206}Pb, ^{207}Pb, ^{208}Pb, ^{238}U, ^{248}ThO, and ^{254}UO), repeated in five scans. The standards D23 and NBS611 were used to identify the position of the peak of mass ^{204}Pb, whereas the calibration of the U content and the Pb/U ratio were done using the zircon standard BR266 (559 Ma, 903 ppm U). Data were reduced using the SQUID© 1.03 software (Ludwig, 2001) and the ages calculated using Isoplot© 3.0 (Ludwig, 2003). The presented ages are mean average $^{206}Pb/^{238}U$ ages calculated at 2σ level, whereas the individual analyses are quoted at 1σ level (Table 2).

6.1.2. Results and evaluation

6.1.2.1. Sample MG44 (meta-quartz-diorite). This meta-quartz-diorite is relatively rich in zircon and about three hundred were recovered from a sample of ± 500 g and 45 of them were placed in an epoxy disc. All grains are medium to long prisms terminated in pyramids (aspect ratio 2:1 to 5:1). The zircon grains are 100–300 μm long, with no evidence both of older inherited cores or zones and of younger metamorphic rim or zones. They have characteristics of magmatic grains such as the zoning and the Th/U ratios averaging 0.61 (see Table 2). An example of dated zircon is provided in Fig. 6, where grain g3 has an age of 471 ± 4 Ma. All grains have ages in the same uncertainty range and all eight analyses group at the $^{206}Pb/^{238}U$ age of 475.7 ± 2.3 Ma (MSWD = 1.8; 2σ)(Fig. 7). This age is considered the age of crystallization of the quartz-diorite body. Metamorphic

Table 2
U–Pb SHRIMP isotopic data of zircon of samples MG44 and MG75a.

Spot	U ppm	Th ppm	Th U	4f206 (%)	Isotopic ratios $^{207}Pb/^{206}Pb$	$^{206}Pb/^{238}U$	$^{207}Pb/^{235}U$	$^{208}Pb/^{232}Th$	Ages $^{207}Pb/^{206}Pb$	$^{206}Pb/^{238}U$	Correl. Coefic.	Disc. %
MG44, meta-quartz-diorite												
g.2-1	240	198	0.85	0.24	0.05573 ± 2.38	0.0759 ± 0.94	0.5830 ± 2.56	0.0232 ± 1.73	442 ± 53	471 ± 4	0.311	−6.8
g.3-1	228	65	0.29	0.00	0.05628 ± 1.41	0.0759 ± 0.94	0.5890 ± 1.69	0.0221 ± 2.09	464 ± 31	471 ± 4	0.482	−1.7
g.4-1	193	124	0.66	0.13	0.05674 ± 1.77	0.0766 ± 0.99	0.5993 ± 2.03	0.0235 ± 1.83	481 ± 39	475 ± 4	0.427	1.1
g.6-1	385	254	0.68	0.16	0.05664 ± 1.49	0.0769 ± 0.84	0.6005 ± 1.71	0.0237 ± 1.37	478 ± 33	477 ± 3	0.404	0.0
g.7-1	260	163	0.65	0.01	0.05612 ± 1.49	0.0772 ± 0.91	0.5977 ± 1.74	0.0240 ± 1.51	457 ± 33	479 ± 3	0.448	−4.9
g.9-1	264	114	0.45	0.07	0.05582 ± 1.36	0.0772 ± 0.91	0.5940 ± 1.64	0.0231 ± 1.67	445 ± 30	479 ± 3	0.480	−7.7
g.10-1	242	125	0.53	0.02	0.05652 ± 1.48	0.0769 ± 1.00	0.5993 ± 1.78	0.0237 ± 1.70	473 ± 33	477 ± 4	0.502	−1.0
g.11-1	108	82	0.79	0.17	0.05532 ± 2.29	0.0763 ± 1.18	0.5821 ± 2.58	0.0233 ± 2.20	425 ± 51	473 ± 5	0.419	−11.5
MG75a, metagabbro												
f.1-1	602	377	0.65	0.50	0.05482 ± 1.98	0.0741 ± 0.94	0.5599 ± 2.19	0.0234 ± 1.70	405 ± 44	461 ± 4	0.431	−14
f.1-2	193	341	1.83	1.25	0.05547 ± 4.67	0.0749 ± 1.29	0.5730 ± 4.85	0.0220 ± 2.04	431 ± 99	466 ± 6	0.267	−8
f.1-3	905	111	0.13	0.04	0.05544 ± 1.51	0.0732 ± 1.01	0.5597 ± 1.82	0.0198 ± 5.62	430 ± 34	456 ± 4	0.556	−6
f.3-1	409	202	0.51	0.07	0.05469 ± 2.52	0.0755 ± 1.00	0.5697 ± 2.71	0.0226 ± 2.59	400 ± 56	469 ± 5	0.369	−17
f.4-1	1034	139	0.14	0.08	0.05554 ± 1.36	0.0728 ± 0.91	0.5577 ± 1.63	0.0200 ± 3.87	434 ± 30	453 ± 4	0.559	−4
f.4-2	1093	123	0.12	0.03	0.05573 ± 1.39	0.0725 ± 0.98	0.5574 ± 1.70	0.0206 ± 5.49	442 ± 31	451 ± 4	0.576	−2
f.4-3	1365	243	0.18	0.06	0.05560 ± 0.80	0.0736 ± 0.92	0.5640 ± 1.22	0.0215 ± 2.04	436 ± 18	458 ± 4	0.758	−5
f.4-4	142	124	0.90	0.43	0.05654 ± 4.08	0.0738 ± 1.19	0.5754 ± 4.25	0.0217 ± 2.75	474 ± 90	459 ± 5	0.279	3
f.5-1	183	743	4.19	3.64	0.05496 ± 3.65	0.0733 ± 1.25	0.5552 ± 3.86	0.0222 ± 1.50	410 ± 82	456 ± 5	0.323	−11
f.8-1	411	288	0.73	0.04	0.05669 ± 1.26	0.0744 ± 1.34	0.5817 ± 1.85	0.0221 ± 1.87	479 ± 28	463 ± 6	0.729	3
f.9-1	597	186	0.32	0.23	0.05330 ± 2.82	0.0753 ± 1.27	0.5537 ± 3.10	0.0216 ± 4.28	342 ± 64	468 ± 6	0.411	−37
f.9-2	520	148	0.29	0.27	0.05615 ± 2.16	0.0762 ± 0.97	0.5902 ± 2.37	0.0239 ± 3.06	458 ± 48	474 ± 4	0.410	−3
f.10-1	286	509	1.84	2.08	0.05579 ± 2.67	0.0748 ± 1.36	0.5751 ± 2.99	0.0218 ± 1.71	444 ± 59	465 ± 6	0.453	−5
f.10-2	278	244	0.91	0.33	0.05594 ± 2.54	0.0768 ± 1.33	0.5923 ± 2.87	0.0236 ± 1.94	450 ± 57	477 ± 6	0.462	−6
f.11-1	266	236	0.92	0.09	0.05266 ± 3.38	0.0750 ± 1.40	0.5444 ± 3.66	0.0224 ± 2.37	314 ± 77	466 ± 6	0.383	−48

Notes: Isotopic ratio errors in %.
All Pb in ratios are radiogenic component corrected for ^{204}Pb.
Disc. = discordance, as 100 − 100{t[$^{206}Pb/^{238}U$]/t[$^{207}Pb/^{206}Pb$]}.
f206 = (common ^{206}Pb)/(total measured ^{206}Pb) based on measured ^{204}Pb.
Uncertainties are 1σ.

conditions probably were not high enough to re-crystallize zircon, so the metamorphic age is not established.

6.1.2.2. MG75a (metagabbro). This metagabbro is relatively poor in zircon only 48 grains were recovered from the rock preparation. Zircon grains are short prisms (aspect ratio 1:1 to 2.5:1) with no pyramid terminations, 50–180 µm long, light-colored, and highly fractured. About 1/3 of the grains show metamorphic rims or areas, which are interpreted as younger than the magmatic areas because they cut magmatic zoning. Only four grains have metamorphic areas large enough to be dated with the SHRIMP spot size of 20–25 µm (grain 1-3, 4-1, 4-2, and 4-3). The metamorphic areas are much brighter in BSE images (Fig. 8), they have higher U contents (average 1099 ppm) and lower Th contents (average Th/U ratios = 0.14) when compared with the darker and zoned magmatic areas (U average = 381 ppm; Th/U average = 0.89) — see Table 2 and Fig. 9b. The U-rich bright areas are interpreted as formed by partial re-crystallization of the zircon under metamorphic conditions, and their ages are about 10 Ma younger than the magmatic phase.

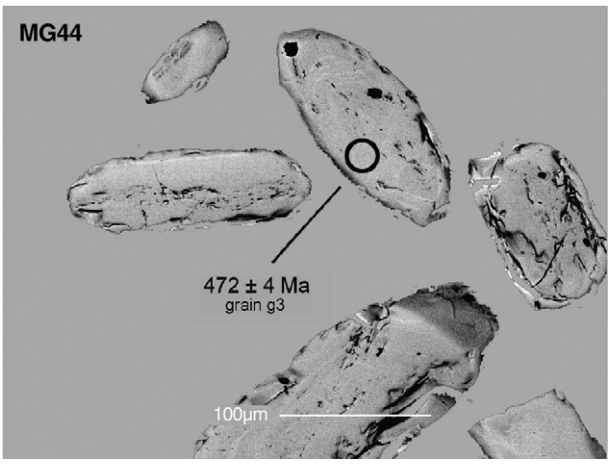

Fig. 6. Back-scattered image of zircon g3, sample MG44 (meta-quartz-diorite).

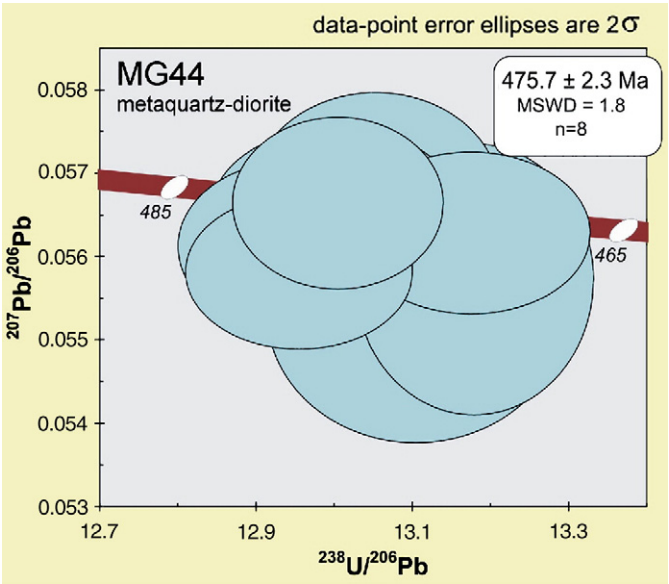

Fig. 7. Inverse concordia plot ($^{207}Pb/^{206}Pb$ versus $^{238}U/^{206}Pb$) of magmatic zircon (sample MG44) providing an age of 475.7 ± 2.3 Ma (MSWD = 1.8; 2σ).

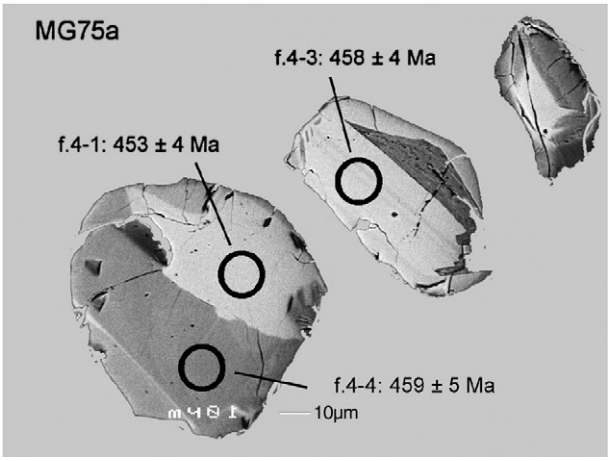

Fig. 8. Back-scattered image of zircon (spots f.4-1, f.4-3, f.4-4), sample MG75a (metagabbro).

The age of the four metamorphic areas is 453.9 ± 2.1 Ma (2 sigma; MSWD = 1.8) using the inverse concordia plot (Fig. 9a), which is similar to the mean average of the $^{206}Pb/^{238}U$ ages (454.5 ± 4.3 Ma; MSWD = 1.7). The age of the magmatic areas is 465.6 ± 3.9 Ma (MSWD of concordance + equivalence = 1.16) using nine out of eleven analyses and calculated at 1 sigma (Fig. 9a). The mean average of the nine $^{206}Pb/^{238}U$ ages is 465.8 ± 3.4 Ma (1 sigma; MSWD = 0.93). Analysis of grain f.5-1 has a very high common lead correction (3.64%) and is not used, whereas analysis f.10-2 is an outlier. Another estimate of the two groups of ages is made using the unmix algorithm (Sambridge and Compston, 1994). Here the metamorphic zircon areas group at 456 ± 1.9 Ma and the magmatic zircon areas at 468 ± 2.3 Ma (relative misfit = 0.592 — Fig. 9c).

6.2. Hf isotopes

6.2.1. Methodology

Hf-isotope analyses were carried out using a New Wave/Merchantek UP213 laser-ablation microprobe, attached to a Nu Plasma multi-collector ICP-MS at GEMOC (Geochemical Evolution and Metallogeny of Continents), Macquarie University, Sydney. Operating conditions include a beam diameter of ~55 µm, a 5 Hz repetition rate, with energy of ~0.4–0.8 mJ. Typical ablation times were 100–120 s, resulting in pits 40–60 µm deep. Mud Tank (MT) zircon was used as reference material which has an average $^{176}Lu/^{177}Hf$ ratio of 0.282522 ± 42 (2SE) (Griffin et al., 2007). MT analyzed in this study was within reported range (0.282514 ± 26; $n = 2$). More detail of the analytical techniques, precision and accuracy is described by Griffin et al. (2000, 2004).

Initial $^{176}Hf/^{177}Hf$ ratios are calculated using measured $^{176}Lu/^{177}Hf$ ratios, with a typical 2 standard error uncertainty on a single analysis of $^{176}Lu/^{177}Hf$ ± 1–2%. Such error reflects both analytical uncertainties and intragrain variation of Lu/Hf typically observed in zircon. Chondritic values of Scherer et al. (2001) (1.865×10^{-11}) have been used for the calculation of e_{Hf} values. Whilst a model of $(^{176}Hf/^{177}Hf)_i = 0.279718$ at 4.56 Ga and $^{176}Lu/^{177}Hf = 0.0384$ has been used to calculate model ages (T_{DM}) based on a depleted mantle source, producing a present-day value of $^{176}Hf/^{177}Hf$ (0.28325) (Griffin et al., 2000, 2004). T_{DM} ages, which are calculated using measured $^{176}Hf/^{177}Hf$ of the zircon, give only the minimum age for the source material from which the original magmas were derived. We have therefore also calculated a "crustal" model age (T^C_{DM}) for each zircon which assumes that the parental magma was produced from an average continental crust ($^{176}Lu/^{177}Hf = 0.015$) that was originally derived from depleted mantle.

6.2.2. Results and evaluation

Five measurements for Hf isotopes were undertaken on four zircon crystals of sample MG75a (metagabbro) (Table 3). All $^{176}Hf/^{177}Hf$ ratios of magmatic and metamorphic areas are similar and the data produced negative ε_{Hf} (from −5.02 to −3.62). The average Lu–Hf model age of the zircon is about 1.7 Ga (Fig. 10). This indicates a crustal contamination of a mantle-derived mafic melt with rocks much older than 1.7 Ga. The negative ε_{Hf} also may indicate that the mafic magma was derived from an enriched mantle subsequently contaminated by crustal components.

7. Geophysics

The studied rocks define a conspicuous aeromagnetic positive anomaly of NNW orientation. It is about 20 km wide in average and

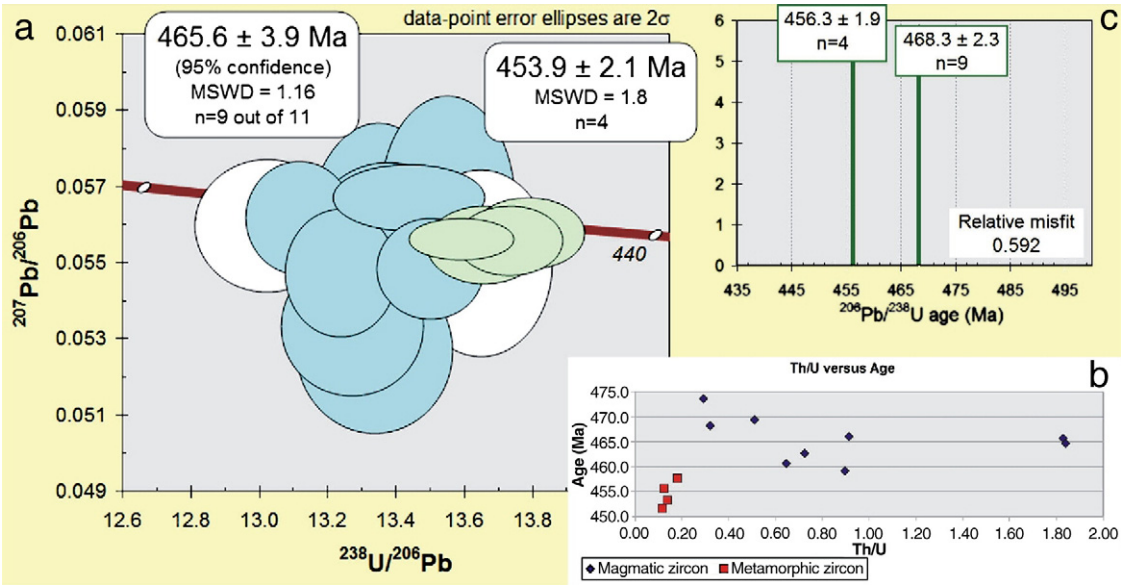

Fig. 9. a) Inverse concordia plot (207Pb/206Pb versus 238U/206Pb) of zircon of sample MG75a. The age of the magmatic areas of zircon provides an age of 465.6 ± 3.9 Ma (MSWD of concordance + equivalence = 1.16; 1 sigma), and the age of the four metamorphic rims/areas calculated at 2 sigma is 453.9 ± 2.1 Ma (MSWD = 1.8). b) Plot of Th/U ratios against the ages of each analysis demonstrating the existence of two groups of ages and two groups of Th/U ratios. c) Deconvolution of the two groups of ages using the mixture modeling algorithm of Sambridge and Compston (1994). The metamorphic zircon crystals group at 456.3 ± 1.9 Ma and the magmatic zircon crystals at 468.3 ± 2.3 Ma (relative misfit = 0.592).

Table 3
Hf isotopic data of four dated zircon of sample MG75a.

	Age	$^{176}Hf/^{177}Hf$	Error	$^{176}Lu/^{177}Hf$	$^{176}Yb/^{177}Hf$	$^{176}Hf/^{177}Hf$	Epsilon	error	T(DM)	T(DM)	Hf Chur	Hf DM
	(Ma)		1SE	±1–2%SE	±1–2%SE	Initial	Hf	1 se	(Ga)	Crustal	(t)	(t)
f.4-1	454±5	0.282342	0.000010	0.000403	0.01661	0.282338	−5.02	0.35	1.22	1.71	0.282480	0.282914
f.4-4	459±5	0.282354	0.000015	0.000753	0.03174	0.282347	−4.66	0.53	1.22	1.69	0.282479	0.282912
f.5-1	456±5	0.282375	0.000013	0.001028	0.04486	0.282366	−4.07	0.46	1.20	1.65	0.282481	0.282914
f.8-1	463±6	0.282340	0.000009	0.000859	0.03655	0.282332	−5.02	0.30	1.24	1.72	0.282474	0.282907
f.10-1	465±6	0.282367	0.000008	0.000657	0.02283	0.282361	−3.62	0.28	1.20	1.65	0.282463	0.282894

Note: ^{176}Lu decay constant = 1.93×10^{-11} (Blichert-Toft and Albarede, 1997).

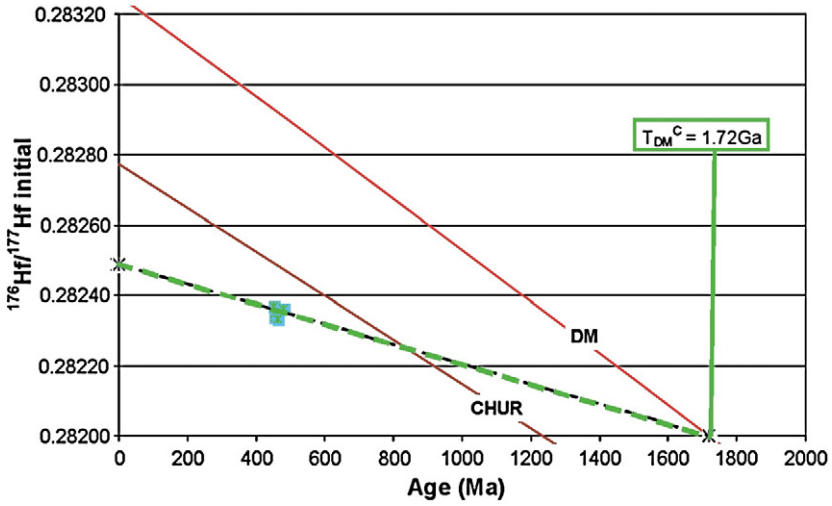

Fig. 10. Plot of $^{176}Hf/^{177}Hf$ ratios versus ages of four dated zircon crystals of sample MG75a (metagabbro). The depleted mantle model age (crustal) is Late Paleoproterozoic (1.7 Ga). The slope of the dashed line uses the ratio of 0.015 for the $^{176}Lu/^{177}Hf$ ratio.

traverses the province of La Pampa in a NNW direction (about 270 km). To the north of 37°S, where there is no aeromagnetic coverage, its continuation is depicted by a positive Bouguer anomaly that broadly follows the same orientation (Fig. 11a). Further to the north, and also along the same NNW corridor, this gravimetric and magnetic anomaly appears at the Sierra de Valle Fertil in the province of San Juan, where its western boundary shows an unusually strong gradient associated with the boundary between Cuyania and Pampia (see Fig. 4, in Introcaso et al., 2004, and Fig. 3d, in Porcher et al., 2004). This anomaly does not extend any further south than about 39°S, where there is a large-scale, roughly E–W, magnetic and gravimetric anomaly thought to represent the northern margin of the Patagonia terrane (see Fig. 5, in Chernicoff and Zappettini, 2004).

A geological interpretation of the aeromagnetic and gravimetric surveys of the area allowed to draw a (pre-Jurassic) basement geological map (Fig. 11b), which represents a substantial improvement with respect to the conventional geological maps available for this region. This map is based on numerous geological and geophysical observations, as well as on extensive radiometric dating and isotopic studies carried out by the authors in the basement of La Pampa province (e.g. Chernicoff and Zappettini, 2004; Chernicoff et al., 2007, 2008a,b,c,d, 2009), together with previous geological information (e.g. Espejo and Silva Nieto, 1996; Tickyj et al., 1999; Melchor and Casadío, 2000; Sato et al., 2000). Six geological units are recognized: 1: undifferentiated Mesoproterozoic (Grenvillian) basement rocks of the Cuyania terrane, 2: Cambro-Ordovician schists/gneisses of the Pampia terrane (host to the Famatinian magmatic arc and back-arc), 3: Ordovician (Famatinian) magmatic arc rocks, 4: Ordovician (Famatinian) magmatic back-arc rocks (belt of MORB-type metagabbros), 5: Upper Ordovician to Devonian marine foreland deposits (depocentre of Curacó basin, sitting on the Cuyania terrane), and 6: Permo-Triassic magmatic rocks (straddling the Cuyania–Pampia terrane divide).

7.1. Modeling the aeromagnetic data

Modeling of the aeromagnetic data was carried out on a 100 km long, roughly E–W transect extracted from the gridded aeromagnetic data, at 250 m sampling interval (see location, in Fig. 11). For the purpose of modeling, the available aeromagnetic data were preferred over the gravimetric data due to their much higher resolution.

From west to east the transect traverses the easternmost Cuyania terrane, the Curacó basin depocentre, the Famatinian magmatic arc, the host basement rocks of the Pampia terrane, a sliver of the Famatinian back-arc and the easternmost basement rocks of the Pampia terrane.

The model suggests that the metaigneous rocks of the Famatinian arc in this profile form a 17 km wide belt, within which a number of narrow (1–4 km) magnetic peaks also occur. It is interpreted that the envelope (low frequency) magnetic anomaly arises from the main, intermediate to acidic rock types of this magmatic belt, and that the more restricted (high frequency), highly magnetic peaks arise from smaller bodies of metagabbro, such as the Urre Lauquen outcrop. This scheme is consistent with the difference in magnetic susceptibility between these rocks, i.e. 0.03 to 0.05 SI (mostly) for the meta-quartz-

Fig. 11. a) Geophysical data of the study region (1: gravimetric data; 2: aeromagnetic data) (see location in Fig. 1). b) Basement geology of the study region, based on limited exposures and geophysical data. ab) location of modeled transect (see Fig. 12).

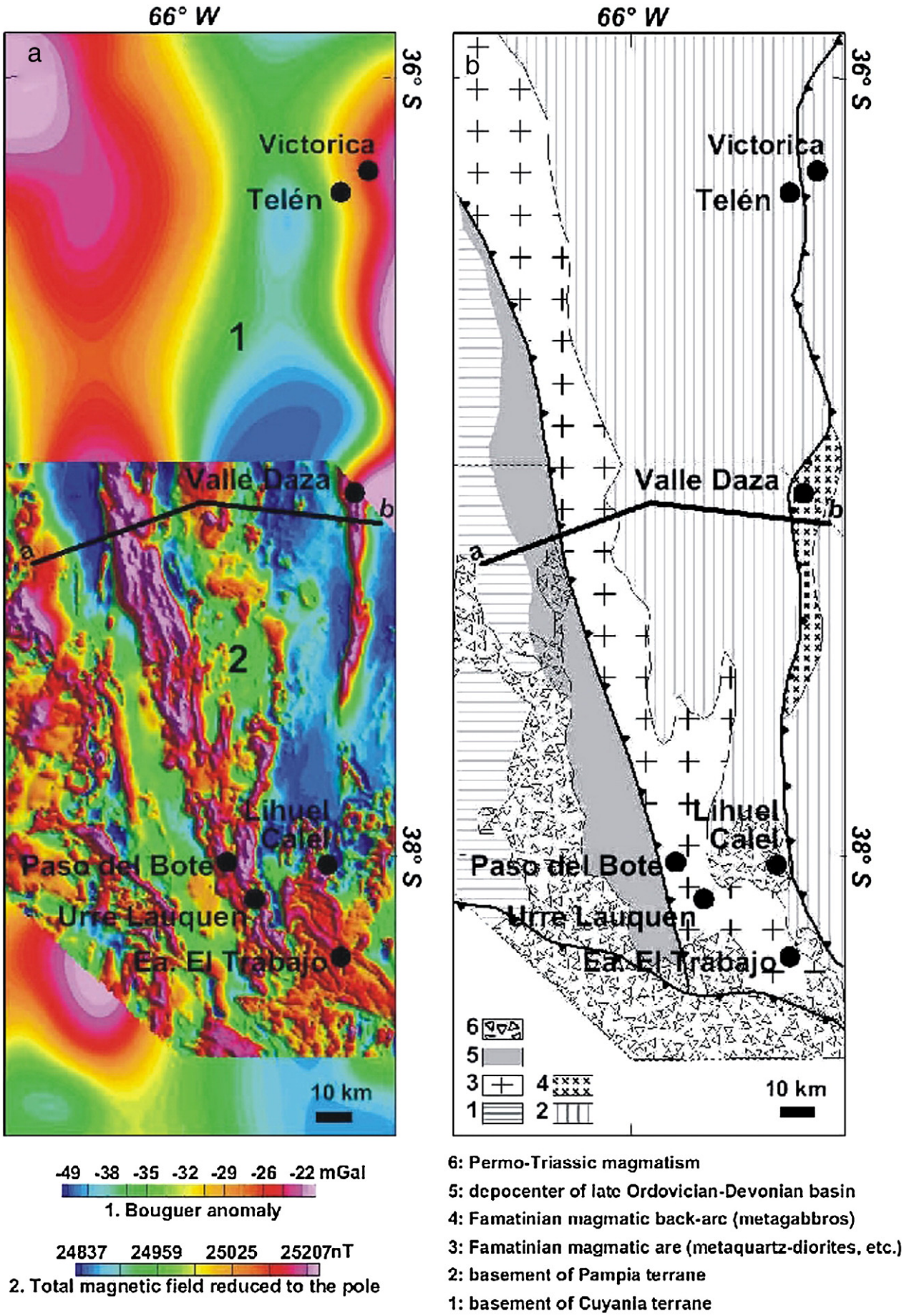

diorites, and 0.09 to 0.10 SI for the metagabbros, which is consistent with the higher magnetite content of the latter. The relative magnetic susceptibilitiy calculated for the flanking Cuyania and Pampia basements is 0.02 SI, that of the sedimentary rocks of the Curacó depocentre is −0.003 SI, that of the Permo-Triassic magmatic rocks is 0.062 SI, and that of the back-arc metagabbros is 0.078 SI.

The geometry of the model (Fig. 12) is consistent with the eastward-dipping subduction leading to the Cuyania–Pampia collision, and the associated synthetic thrusts. It also accounts for the predominance of Middle Ordovician metamorphic zircon (derived from the Famatinian orogen) found in the adjacent Curacó basin (Chernicoff et al., 2008d).

8. Discussion

In south-central Argentina (La Pampa province) – a flat region mostly covered by Quaternary sediments – the presence of a large and conspicuous NNW-trending aeromagnetic anomaly helped recognize an almost completely hidden segment of the Famatinian magmatic arc which, otherwise, is well exposed in central and northern Argentina.

Only a small portion of this aeromagnetic anomaly can be directly attributed to the limited exposures of the metaigneous rocks at Paso del Bote, Urre Lauquen and Estancia El Trabajo. The physical continuity of the anomaly to the north suggests that its full extent originates from similar, unexposed, metaigneous rocks, forming a single NNW-trending belt.

The magmatic suite has a calc-alkaline trend, and is enriched in light REE resulting from crustal contamination. Its geochemical signature also points to a pre-collisional magmatic arc developed in the continental crust. This suite plots largely in coincidence with those of the central and northern segments of the Famatinian arc, both showing similar characteristics such as their metaluminous character, subalkaline pattern, calc-alkaline evolution trend, arc-type magmatism and LREE enrichment.

The metagabbros of this suite are subalkaline arc tholeiites contaminated by a crustal source as indicated by the Hf isotopes. They differ from the MORB-type metagabbros of Valle Daza and Sierra de Lonco Vaca (located ca. 50 km to the east, also in La Pampa province, Figs. 1 and 11b) regarded to belong to the Famatinian magmatic back-arc (Chernicoff et al., 2008c, 2009). Similar, subalkaline arc-type gabbros have been found at Sierra de Chepes (central Sierras Pampeanas; Pankhurst et al., 1998), displaying metaluminous character, low alkali content (<3%) and flat REE patterns with no Eu anomalies.

The crystallization ages of the metaigneous rocks of the study area range from 475.7 ± 2.3 Ma (meta-quartz-diorites) to 465.6 ± 3.9 Ma (metagabbros), as established by U–Pb SHRIMP dating on magmatic zircon. The Hf-isotope composition of the dated zircon of the metagabbro indicates model ages around 1.7 Ga, which are results of a mixture of a mafic magma of ca. 466 Ma with a much older crustal component, probably older than 2 Ga. This strongly suggests that part of the underlying basement of the southernmost Pampia terrane is at least this old.

U–Pb SHRIMP dating on metamorphic zircon rims/areas of the metagabbros yielded 453.9 ± 2.1 Ma. This age of metamorphism falls within the range of ages of Famatinian metamorphism previously recorded in the basement rocks of La Pampa (i.e. ca. 465 Ma in the metasedimentary host rocks, Chernicoff et al., 2008a; ca. 450 Ma in the back-arc metagabbros of Valle Daza, Chernicoff et al., 2008c; ca. 466 Ma in detritic metamorphic zircon from the Curacó Basin, Chernicoff et al., 2008d), as well as in the 460–450 Ma peak age of metamorphism of the basement rocks closest to the present study area exposed in the Sierra de San Luis (Sims et al., 1998).

As a whole, the timing of the Famatinian arc magmatism and regional metamorphism in La Pampa is comparable to those of other segments of the Famatinian arc, e.g. Sierra de San Luis, central Sierras Pampeanas, Sierra de Famatina and Puna (Faja Eruptiva Occidental, of northwestern Argentina–Chile) (Fig. 13).

In the Sierra de San Luis, the Famatinian magmatic arc was active since Middle Cambrian times, with a climax during the Ordovician (see López de Luchi et al., 2007, for an updated list of the available ages); regional metamorphism in the Sierra de San Luis has been reported to span from 480 to 445 Ma (e.g. Sato et al., 2003, and references therein).

In the central Sierras Pampeanas (Los Llanos-Ulapes, Chepes), the bulk of the arc magmatism occurred at ca. 490 Ma, and recurred at ca. 470 Ma, persisting until ca. 450 Ma (Pankhurst et al., 1998).

In the central Sierra de Famatina, the Nuñorco granite yielded ca. 460 Ma.(U–Pb zircon; Loske and Miller, 1996), and in the western Sierra de Famatina the metaluminous granitoids of cerro Asperecito were dated at ca. 468 Ma (Rapela et al., 1999; Pankhurst et al., 2000). Dahlquist et al. (2008) have recently dated the granitoids of the central-west Sierra de Famatina at 481 ± 4 to 463 ± 4 Ma (U–Pb SHRIMP).

Some of the several dated exposures of the Argentine segment of the Faja Eruptiva Occidental (Puna region) include, e.g., the Taca Taca Granite (476 ± 7 Ma, U–Pb on zircon; Makepeace et al., 2002), the Sierra de Macón granitoids (482.7 ± 7.8 Ma, Ar/Ar on hornblende; Koukharsky et al., 2002), the Pocitos eruptive complex (494 ± 20 and 470 ± 17 Ma, K/Ar on hornblende; Blasco and Zappettini, 1996), and the Quebrada Caballo Muerto-Archibarca granitoids (485 ± 15 Ma, K/Ar on biotite; Palma et al., 1986).

In the Chilean portion of the Faja Eruptiva Occidental, the Famatinian volcanics of the Cordón La Lila Complex have a minimum age of ca. 429 Ma (Mpodozis et al., 1983), the age of the Choschas pluton is poorly constrained (487 ± 50 Ma and 467 ± 50 Ma, Pb alpha dates; Mpodozis et al., 1983), the Alto del Inca pluton is dated 478 ± 44 Ma (Rb–Sr whole rock, Mpodozis et al., 1983), the Tilopozo pluton is dated 452 ± 4 (Rb–Sr whole rock, Mpodozis et al., 1983), and the Tucúraco pluton yielded 441 ± 8 Ma (Rb–Sr whole rock, Mpodozis et al., 1983).

The amphibolite-facies metamorphism that affects the magmatic arc in La Pampa is attributed to the effects derived from the collision of Cuyania. The overprinted ductile deformation under greenschist-facies metamorphic conditions could be interpreted as syn-tectonic shearing parallel to the Pampia–Cuyania suture, consistent with that described further north in the type localities of the Famatinian granitoids. The Devonian orogenic phase (or Achalian orogeny, of Sims et al., 1998), thought to be related to the collision of Chilenia to the west, could have reactivated the shear zones. Lastly, the evidence of mineralization and hydrothermal alteration could be assigned to the widespread Permo-Triassic magmatism present in the study region that includes genetically related ore deposits such as the Lihuel Calel Cu mine (see Fig. 1). The absence of metamorphic minerals in the dikes that are emplaced parallel to the foliation of the metaigneous rocks at Paso del Bote is indicative of their post-tectonic origin, hence their possible Permo-Triassic age cannot be precluded. Granodiorites to monzogranites from Estancia El Trabajo are, on the whole, less affected by metamorphism, indicating their late tectonic stage emplacement.

Similarly to the other segments of the Famatinian arc, the metaigneous rocks of the present study area lie on the Pampia (Gondwana) side (upper plate) of the Cuyania–Pampia suture zone, in agreement with the early Paleozoic east-dipping subduction of Iapetan oceanic lithosphere beneath the proto-Andean margin of western Gondwana.

Immediately west of the suture, lying on Cuyanian crust, is the depocentre of a Late Ordovician–Devonian marine foreland basin generated after the collision of Cuyania (Curacó basin, Chernicoff et al., 2008d) (Fig. 11b). Geochemical signature of its sedimentary fill indicates derivation from an active continental margin, possibly corresponding to the Famatinian arc.

Fig. 14 depicts the model for the evolution envisaged for the Famatinian arc–back-arc system in south-central Argentina. The studied metaigneous rocks of La Pampa are regarded to represent the

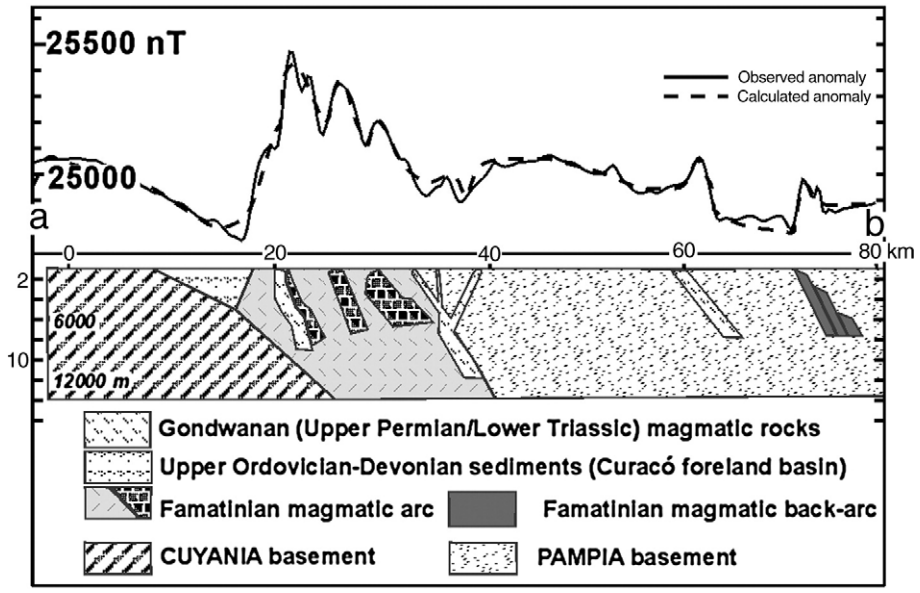

Fig. 12. Schematic model of the aeromagnetic data (see location of transect in Fig. 11).

southernmost occurrence of the Famatinian magmatic arc, terminating at the northern margin of the Patagonia terrane. Although there is evidence of Ordovician magmatism and metamorphism in eastern Patagonia at ca. 470 Ma (zircon U–Pb SHRIMP dating; Pankhurst et al., 2001), this is most probably related to an independent orogen, in accordance with either the originally proposed allochthonous nature of the Patagonia terrane (Ramos, 1984) or its more recently proposed para-autochthonous nature (Rapalini, 2005; Ramos, 1998).

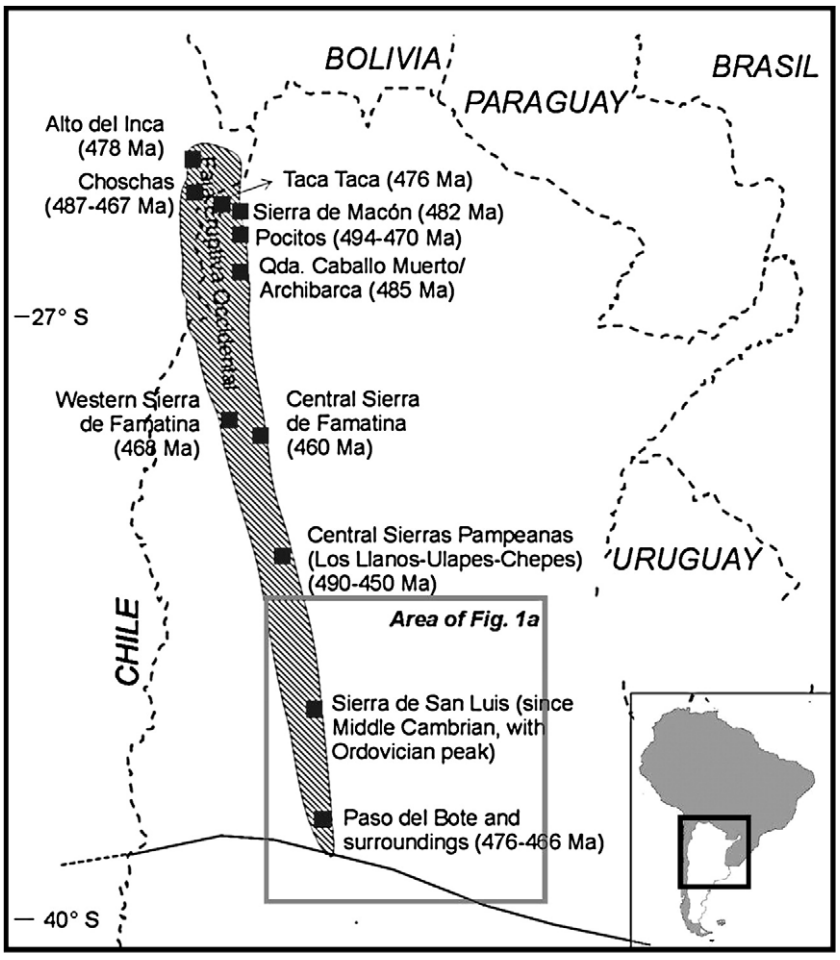

Fig. 13. Areal extent of the Famatinian magmatic arc (hatched area) and main outcrops with indication of age. (See location, in Fig. 1).

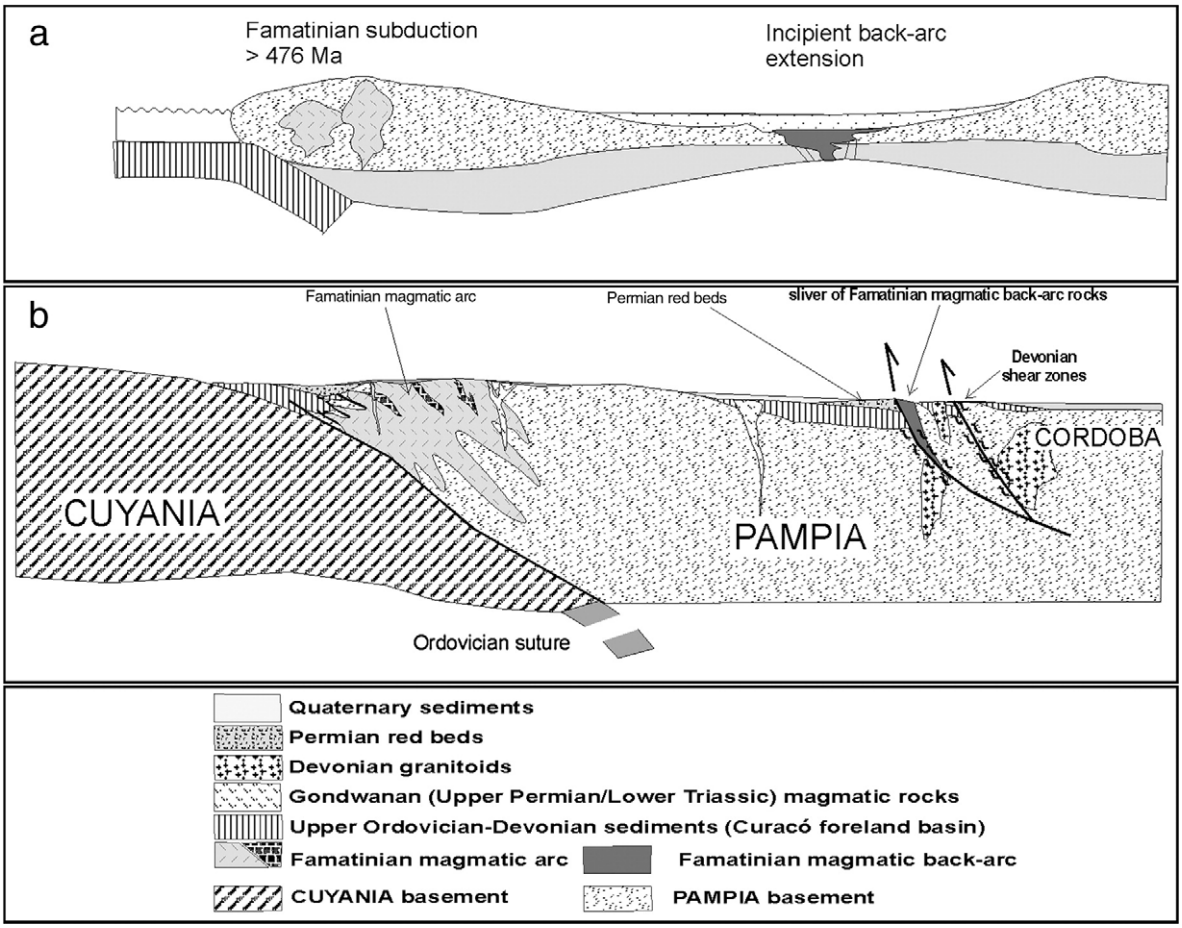

Fig. 14. Schematic model of the evolution of the Famatinian magmatic arc–back-arc system in south-central Argentina (La Pampa province). a) early development of continental magmatic arc (>476 Ma); b) Cenozoic configuration of the region.

Acknowledgements

This work received financial support from Research Grant PIP5008 (CONICET, Council for Scientific and Technical Research of Argentina). The Geological Survey of Argentina (SEGEMAR) provided logistical support and geophysical data. Two anonymous reviews helped improve the quality of this article.

References

Astini, R.A., Dávila, F.M., 2004. Ordovician back arc foreland and Ocloyic thrust belt development on the western Gondwana margin as a response to Precordillera terrane accretion. Tectonics 23, TC4008. doi:10.1029/2003TC001620.

Astini, R.A., Benedetto, J.L., Vaccari, N.E., 1995. The early Paleozoic evolution of the Argentine Precordillera as a Laurentia rifted, drifted, and collided terrane: a geodynamic model. Geological Society of America Bulletin 107 (253), 274.

Astini, R.A., Ramos, V.A., Benedetto, J.L., Vaccari, N.E., Cañas, F.L., 1996. La Precordillera: un terreno exótico a Gondwana. 13 Congreso Geológico Argentino and 3 Congreso de Exploración de Hidrocarburos, Actas, vol. 5, pp. 293–324. Buenos Aires.

Bahlburg, H., 1998. The geochemistry and provenance of Ordovician turbidites in the Argentine Puna. In: Pankhurst, R.J., Rapela, C.W. (Eds.), The Proto-Andean Margin of Gondwana: Geological Society, London, Special Publication, vol. 142, pp. 127–142.

Baldo, E., Casquet, C., Rapela, C.W., Pankhurst, R.J., Galindo, C., Fanning, C.M., Saavedra, J., 2001. Ordovician metamorphism at the southwestern margin of Gondwana: P-T conditions and U–Pb SHRIMP ages from the Loma de Las Chacras, Sierras Pampeanas. Third South American Symposium of Isotope Geology, Pucón, Chile, SERNAGEOMIN, Santiago, pp. 544–547.

Blasco, G., Zappettini, E., 1996. Hoja geológica San Antonio de los Cobres. 2566-1, Programa Nacional de Cartas Geológicas 1:250.000, Boletín 217. Servicio Geológico Minero Argentino, Buenos Aires. 126 pp.

Blichert-Toft, J., Albarede, F., 1997. The Lu–Hf isotope geochemistry of chondrites and the evolution of the mantle–crust system. Earth Planetary Science Letters 148, 243–258.

Casquet, C., Baldo, E., Pankhurst, R.J., Rapela, C.W., Galindo, C., Fanning, C.M., Saavedra, J., 2001. Involvement of the Argentine Precordillera terrane in the Famatinian Mobile Belt: geochronological (U–Pb SHRIMP) and metamorphic evidence from the Sierra de Pie de Palo. Geology 29, 703–706.

Casquet, C., Pankhurst, R.J., Vaughan, A.P.M., 2008. The West Gondwana margin: Proterozoic to Mesozoic. Gondwana Research 13, 147–149.

Chernicoff, C.J., Zappettini, E.O., 2003. Delimitación de los terrenos tectonoestratigráficos de la región centro-austral argentina: evidencias aeromagnéticas. Revista Geológica de Chile 30 (2), 299–316.

Chernicoff, C.J., Zappettini, E., 2004. Geophysical evidence for terrane boundaries in south-central Argentina: Gondwana research 7, 1105–1116.

Chernicoff, C.J., Santos, J.O.S., Zappettini, E.O., McNaughton, N.J., 2007. Esquistos del Paleozoico Inferior en la cantera Green, sur de San Luis, Argentina: edades U–Pb SHRIMP e implicancias geodinámicas. Revista Asociación Geológica Argentina 62 (1), 154–158.

Chernicoff, C.J., Santos, J.O.S., Zappettini, E.O., McNaughton, N.J., 2008a. U–Pb SHRIMP dating of the Famatinian (Lower Paleozoic) metamorphism in La Pampa province, Argentina. 6 South American Symposium on Isotope Geology, Proceedings on CD: article No. 8: 5 pages. San Carlos de Bariloche.

Chernicoff, C.J., Santos, J.O.S., Zappettini, E.O., McNaughton, N.J., 2008b. Zircon U–Pb SHRIMP dating of Lower Paleozoic paraschists at sierra de Lonco Vaca, La Pampa province, Argentina. 6 South American Symposium on Isotope Geology, Proceedings on CD: article No. 9: 4 pages. San Carlos de Bariloche.

Chernicoff, C.J., Santos, J.O.S., Zappettini, E.O., Villar, L.M., McNaughton, N.J., 2008c. Zircon U–Pb SHRIMP dating of the Lower Paleozoic La Pampa belt of metagabbros, Argentina. 6 South American Symposium on Isotope Geology, Proceedings on CD: article No. 7: 6 pages. San Carlos de Bariloche.

Chernicoff, C.J., Zappettini, E.O., Santos, J.O.S., Beyer, E., McNaughton, N.J., 2008d. Foreland basin deposits associated with Cuyania terrane accretion in La Pampa province, Argentina. Gondwana Research 13 (2), 189–203.

Chernicoff, C.J., Zappettini, E.O., Santos, J.O.S., Villar, L.M., McNaughton, N.J., 2008e. El arco magmático famatiniano en la provincia de La Pampa. 17 Congreso Geológico Argentino, Actas: 11–12. San Salvador de Jujuy.

Chernicoff, C.J., Zappettini, E.O., Villar, L.M., Chemale, F., Hernández, L., 2009. The belt of metagabbros of La Pampa: Lower Paleozoic back-arc magmatism in south-central Argentina. Journal of South American Earth Sciences 28 (4), 383–397.

Coira, B., Koukharsky, M., 2002. Ordovician volcanic activity in the Puna, Argentina. In: Aceñolaza, F.G. (Ed.), Aspects of the Ordovician System in Argentina: Instituto Superior de Correlación Geológica, Serie Correlación Geológica, vol. 16, pp. 267–280. Tucumán.

Cox, K.G., Bell, J.D., Pankhurst, R.J., 1979. The Interpretation of Igneous Rocks. George, Allen and Urwin, London.
Dahlquist, J.A., Pankhurst, R.J., Rapela, C.W., Galindo, P., Alasino, C.M., Fanning, J., Saavedra, J., Baldo, E., 2008. New SHRIMP U–Pb data from the Famatina Complex: constraining Early–Mid Ordovician Famatinian magmatism in the Sierras Pampeanas, Argentina. Geologica Acta 4, 319–333.
Espejo, P.M., Silva Nieto, D.G., 1996. Hoja Geológica 3966-II Puelches. Programa Nacional de Cartas Geológicas 1:250.000. Dirección Nacional del Servicio Geológico. Buenos Aires. Boletín 216, 1–35.
Green, T.H., Watson, E.B., 1982. Crystallization of apatite in natural magmas under high pressure, hydrous conditions, with particular reference to 'orogenic' rock series. Contributions to Mineralogy and Petrology 79, 96–105.
Gregori, D.A., Kostadinoff, J., Strazzere, L., Raniolo, A., 2008. Tectonic significance and consequences of the Gondwanie orogeny in northern Patagonia, Argentina. Gondwana Research 14, 429–450.
Griffin, W.L., Pearson, N.J., Belousova, E.A., Jackson, S.R., van Achterbergh, E., O'Reilly, S.Y., Shee, S.R., 2000. The Hf isotope composition of cratonic mantle: LAM-MC-ICPMS analysis of zircon megacrysts in kimberlites. Geochimica et Cosmochimica Acta 64, 133–147.
Griffin, W.L., Belousova, E.A., Shee, S.R., Pearson, N.J., O'Reilly, S.Y., 2004. Archean crustal evolution in the northern Yilgarn Craton: U–Pb and Hf-isotope evidence from detrital zircons. Precambrian Research 131, 231–282.
Griffin, W.L., Pearson, N.J., Belousova, E.A., Saeed, A., 2007. Reply to "Comment to short-communication 'Comment: Hf-isotope heterogeneity in zircon 91500' by W.L. Griffin, N.J. Pearson, E.A. Belousova and A. Saeed (Chemical Geology 233 (2006) 358–363)" by F. Corfu. Chemical Geology 244, 354–356.
Introcaso, A., Martinez, M.P., Gimenez, M.E., Ruiz, F., 2004. Geophysical study of the Valle Fértil Lineament between 28°45´S and 31°30´S: boundary between the Cuyania and Pampia terranes. Gondwana Research 7 (4), 1117–1132.
Irvine, T.N., Baragar, W.R.A., 1971. A guide to the chemical classification of the common volcanic rocks. Canadian Journal of Earth Sciences 8, 523–548.
Koukharsky, M.L., Quenardelle, S., Litvak, V., Maisonnave, E.B., Page, S., 2002. Plutonismo del ordovícico inferior en el sector norte de la sierra de Macon, provincia de Salta. Asociación Geológica Argentina, Revista 57 (2), 173–181.
López de Luchi, M.G., Siegesmund, S., Wemmer, K., Steenken, A., Naumann, R., 2007. Geochemical constraints on the petrogenesis of the Palaeozoic granitoids of the Sierra de San Luis, Sierras Pampeanas, Argentina. Journal of South American Earth Sciences 24 (2–4), 138–166.
Loske, W., Miller, H., 1996. Sistemática U–Pb de circones del granito de Ñuñorco-Sañogasta. In: Aceñolaza, F.G., Miller, H., Toselli, A. (Eds.), Geología del Sistema de Famatina: Münchner Geologische Hefte, vol. 19(A), pp. 221–227. München.
Ludwig, K.R., 2001. Squid 1.02: A Users Manual. Berkeley Geochronology Centre, Special Publication No. 2. 19 pp.
Ludwig, K.R., 2003. Isoplot 3.00, a geochronological tool-kit for Excel. Berkeley Geochronology Center Special Publication, vol. 4. 67 pp.
Makepeace, A., Stasiuk, M., Krauth, O., Hickson, C., Cocking, R., Ellerbeck, M., 2002. Muiltinational Andean Project. Geodata CD-ROM. Publicación Geológica Multinacional, vol. 3. SERNAGEOMIN, Santiago.
McDonough, W.F., Sun, S., 1995. The composition of the Earth. Chemical Geology 120, 223–253.
Melchor, R., Casadío, S., 2000. Hoja Geológica 3766-III La Reforma, provincia de La Pampa. Programa Nacional de Cartas Geológicas 1:250.000. Servicio Geológico Minero Argentino, Buenos Aires, Boletin 295, 1–71.
Mpodozis, C., Hervé, F., Davidson, J., Rivano, S., 1983. Los granitoides de Cerro Lila, manifestaciones de un episodio intrusivo y termal del Paleozoico inferior en los Andes del norte de Chile. Revista Geológica de Chile 18, 3–14.
Palma, M.A., Parica, P.D., Ramos, V.A., 1986. El granito Archibarca: su edad y significado tectónico, provincia de Catamarca. Asociación Geológica Argentina, Revista 41 (3/4), 414–419.
Pankhurst, R.J., Rapela, C.W., 1998. Introduction. In: Pankhurst, R.J., Rapela, C.W. (Eds.), The Proto-Andean Margin of Gondwana: Geological Society of London, Special Publications, vol. 142, pp. 1–10. London.
Pankhurst, R.J., Rapela, C.W., Saavedra, J., Baldo, E., Dahlquist, J., Pascua, I., Fanning, C.M., 1998. The Famatinian magmatic arc in the central Sierras Pampeanas: an Early to Mid-Ordovician continental arc on the Gondwana margin. In: Pankhurst, R.J., Rapela, C.W. (Eds.), The Proto-Andean Margin of Gondwana: Geological Society of London, Special Publications, vol. 142, pp. 343–367. London.
Pankhurst, R.J., Rapela, C.W., Fanning, C.M., 2000. Age and origin of coeval TTG, I- and S-type granites in the Famatinian belt of NW Argentina. Transactions of the Royal Society of Edinburgh: Earth Sciences 91, 151–168.
Pankhurst, R.J., Rapela, C.W., Fanning, C.M., 2001. The Mina Gonzalito Gneiss: Early Ordovician Metamorphism in Northern Patagonia. 3° South American Symposium on Isotope Geology: Actas Electrónicas Sesion, vol. 6(4), pp. 1–4. Pucón.
Pearce, J.A., Harris, N.B.W., Tindle, A.G., 1984. Trace element discrimination diagrams for the tectonic interpretation of granitic rocks. Journal of Petrology 25, 956–983.
Poma, S., Zappettini, E., 1998. El magmatismo paleozoico de la Puna Occidental, provincia de Salta, Argentina. 10 Congreso Latinoamericano de Geología. Actas II, pp. 306–313. Buenos Aires.
Poma, S., Quenardelle, S., Litvak, V., Maisonnave, E.B., Koukharsky, M., 2004. The Sierra de Macon, Plutonic expression of the Ordovician magmatic arc, Salta Province Argentina. Journal of South American Earth Sciences 16, 587–597.
Porcher, C.C., Fernandes, L.A.D., Vujovich, G.I., Chernicoff, C.J., 2004. Thermobarometry, Sm/Nd ages and geophysical evidence for the location of the suture zone between Cuyania and the western proto-Andean margin of Gondwana. Gondwana Research 7 (4), 1057–1076.
Quenardelle, S.M., Ramos, V.A., 1999. Ordovician western Sierras Pampeanas magmatic belt: record of Precordillera accretion in Argentina. In: Ramos, V.A., Keppie, D. (Eds.), Laurentia Gondwana Connections before Pangea: Geological Society of America, Special Paper, vol. 336, pp. 63–86.
Ramos, V.A., 1984. Patagonia: un continente paleozoico a la deriva? 9° Congreso Geológico Argentino (Bariloche), Actas, vol. 2, pp. 311–325. Buenos Aires.
Ramos, V.A., 1996. Evolución tectónica de la Plataforma Continental. In: Ramos, V.A., Turic, M.A. (Eds.), Geología y Recursos Naturales de la Plataforma Continental Argentina. Asociación Geológica Argentina / Instituto Argentino del Petróleo, pp. 385–404. Buenos Aires.
Ramos, V.A., 1998. Patagonia: a Paleozoic continent adrift? Journal of South American Earth Sciences 26 (3), 235–251.
Ramos, V.A., 2004. Cuyania, an exotic block to Gondwana: review of a historical success and the present problems. Gondwana Research 7 (4), 1009–1026.
Rapalini, A.E., 2005. The accretionary history of southern South America from the latest Proterozoic to the Late Paleozoic: some paleomagnetic constraints. In: Vaughan, A. P.M., Leat, P.T., Pankhurst, R.J. (Eds.), Terrane Processes at the Margins of Gondwana: Geological Society, London, Special Publications, vol. 246, pp. 305–328.
Rapela, C.W., Pankhurst, R.J., Casquet, C., Baldo, E., Saavedra, J., Galindo, C., Fanning, C.M., 1998. The Pampean orogeny of the southern proto-Andes: Cambrian continental collision in the Sierras de Córdoba. In: Pankhurst, R., Rapela, C. (Eds.), The Proto-Andean Margin of Gondwana: Geological Society of London, Special Publications, vol. 142, pp. 181–217. London.
Rapela, C.W., Pankhurst, R.J., Dahlquist, J., Fanning, C.M., 1999. U–Pb SHRIMP ages of Famatinian granitoid: new constraints on the timing, origin and tectonic setting of I- and S-type magmas in an ensialic arc. 2º South American Symposium on Isotope Geology (Villa Carlos Paz), Actas, pp. 264–267.
Rapela, C.W., Pankhurst, R.J., Baldo, E., Casquet, C., Galindo, C., Fanning, C.M., Saavedra, J., 2001. Ordovician metamorphism in the Sierras Pampeanas: new U–Pb SHRIMP ages in central-east Valle Fértil and the Velasco Batholith. Third South American Symposium of Isotope Geology, Pucón, Chile, SERNAGEOMIN, Santiago, pp. 616–619.
Saavedra, J., Pellitero, E.P., Rossi, J.N., Toselli, A.J., 1992. Magmatic evolution of the Cerro Toro granite, a complex Ordovician pluton of northwestern Argentina. Journal of South American Earth Sciences 5 (1), 21–32.
Sambridge, M.S., Compston, W., 1994. Mixture modelling of multi-component data sets with application to ion-probe zircon ages. Earth and Planetary Science Letters 128, 373–390.
Sato, A.M., Tickyj, H., Llambías, E.J., Sato, K., 2000. The Las Matras Tonalitic–Trondhjemitic pluton, central Argentina: Grenvillian age constraints, geochemical characteristics and regional implications. Journal of South American Earth Sciences 13, 587–610.
Sato, A.M., González, P.D., Llambías, E.J., 2003. Evolución del orógeno Famatiniano en la Sierra de San Luis: magmatismo de arco, deformación y metamorfismo de bajo a alto grado. Revista Asociación Geológica Argentina 58 (4), 487–504.
Scherer, E., Münker, C., Mezger, K., 2001. Calibration of the lutetium–hafnium clock. Science 293 (5530), 683–687.
SEGEMAR, 2005. Aeromagnetic survey of La Pampa, Argentina: digital data. Servicio Geológico-Minero Argentino.
Shervais, J.W., 1982. Ti–V plots and the petrogenesis of modern and ophilitic lavas. Earth and Planetary Science Letters 59, 101–118.
Sims, J.P., Ireland, T.R., Camacho, A., Lyons, P, Skirrow, R.G., Stuart-Smith, P.G., Miró, R., 1998. U–Pb, Th–Pb and Ar–Ar geochronology from southern Sierras Pampeanas, Argentina: implications for the Palaeozoic tectonic evolution of the western Gondwana margin. In: Pankhurst, R.J., Rapela, C.W. (Eds.), The Proto-Andean Margin of Gondwana: Geol. Soc. London, Spec. Pub., vol. 142, pp. 235–258.
Stuart-Smith, P.G., Camacho, A., Sims, J.P., Skirrow, R.G., Lyons, P., Pieters, P.E., Black, L.P., Miró, R., 1999. Uranium–lead dating of felsic magmatic cycles in the southern Sierras Pampeanas, Argentina: implications for the tectonic development of the proto-Andean Gondwana margin. In: Ramos, V.A., Keppie, J.D. (Eds.), Laurentia–Gondwana before Pangea: Geological Society of America Special Paper, vol. 336, pp. 87–114.
Thomas, W.A., Astini, R.A., 2003. Ordovician accretion of the Argentine Precordillera terrane to Gondwana: a review. Journal of South American Earth Sciences 16, 67–79.
Tickyj, H., Llambías, E.J., Sato, A.M., 1999. El basamento cristalino de la región suroriental de la provincia de La Pampa: extensión austral del Orógeno Famatiniano de Sierras Pampeanas. 14 Congreso Geológico Argentino, Actas, vol. I, pp. 160–163. Buenos Aires.
Toselli, A.J., Sial, A.N., Rossi, J.N., 2002. Ordovician magmatism of the Sierras Pampeanas, Famatina System and Cordillera Oriental, NW Argentina. In: Aceñolaza, F.G. (Ed.), Aspects of the Ordovician System in Argentina: Instituto Superior de Correlación Geológica, Serie Correlación Geológica, vol. 16, pp. 313–326. Tucumán.
Varela, R., Basei, M.A.S., Pereyra, C.P., 2008. Datación U–Pb del granito Paimán, sierra de Paimán, Chilecito, La Rioja. Revista Asociación Geológica Argentina 63 (1), 97–101.
Villar, L.M., Chernicoff, C.J., Zappettini, E.O., 2005. Evidence of a Famatinian continental magmatic arc at Paso del Bote, La Pampa province, Argentina. Gondwana 12 Conference. Mendoza. Actas, p. 365.
Von Gosen, W., Loske, W., Prozzi, C., 2002. New isotopic dating of intrusive rocks in the Sierra de San Luis (Argentina): implications for the geodynamic history of the Eastern Sierras Pampeanas. Journal of South American Earth Sciences 15 (2), 237–250.
Vujovich, G.I., van Staal, C.R., Davis, W., 2004. Age constrains on the tectonic evolution and provenance of the Pie de Palo Complex, Cuyania composite terrane, and the Famatinian orogeny in the sierra de Pie de Palo, San Juan, Argentina. Gondwana Research 7 (4), 1041–1056.
Wilson, M., 1989. Igneous Petrogenesis. Irwin Hyman, London. 466 pp.
Wood, D.A., 1980. The application of Th–Hf–Ta diagram to problems of tectonomagmatic classification and to establishing the nature of crustal contamination of basaltic lavas of the British Tertiary volcanic province. Earth and Planetary Science Letters 50, 11–30.
Zimmermann, U., Bahlburg, H., 2003. Provenance analysis and tectonic setting of the Ordovician deposits in the southern Puna basin, NW Argentina. Sedimentology 50, 1079–1104.